1-1-2013

Comparison Of Denitrification Potential Around A Tile Drain And In Aquifer Sediments: Oakes, ND

Chase Christenson

COMPARISON OF DENITRIFICATION POTENTIAL AROUND A TILE DRAIN AND IN AQUIFER SEDIMENTS: OAKES, ND.

by

Chase Joseph Christenson
Bachelor of Science, University of North Dakota, 2008

A Thesis

Submitted to the Graduate Faculty

of the

University of North Dakota

In partial fulfillment of the requirements

for the degree of

Master of Science

Grand Forks, North Dakota
May
2013

This thesis, submitted by Chase J. Christenson in partial fulfillment of the requirements for the Degree of Master of Science from the University of North Dakota, has been read by the Faculty Advisory Committee under whom the work has been done, and is hereby approved.

Dr. Scott Korom

Dr. Philip Gerla

Dr. Richard Lefever

This thesis is being submitted by the appointed advisory committee as having met all of the requirements of the Graduate School at the University of North Dakota and is hereby approved.

Dr. Wayne Swisher
Dean of the Graduate School

April 30, 2013
Date

PERMISSION

Title: Comparison of Denitrification Potential around a Tile Drain and in Aquifer Sediments: Oakes, ND

Department: Geology

Degree: Master of Science

In presenting this thesis in partial fulfillment of the requirements for a graduate degree from the University of North Dakota, I agree that the library of this University shall make it freely available for inspection. I further agree that permission for extensive copying for scholarly purposes may be granted by the professor who supervised my thesis work or, in his absence, by the Chairperson of the department or the dean of the Graduate School. It is understood that any copying or publication or other use of this thesis or part thereof for financial gain shall not be allowed without my written permission. It is also understood that due recognition shall be given to me and to the University of North Dakota in any scholarly use which may be made of any material in my thesis.

Chase J. Christenson
April 22, 2013

TABLE OF CONTENTS

LIST OF FIGURES

Figure Page

LIST OF TABLES

ACKNOWLEDGMENTS

Without the unfailing patience and support from my committee chairman, Dr. Scott Korom, during my undergraduate and graduate career this work would have gone unfinished. I would also like to thank the other members of my committee; Dr. Philip Gerla and Dr. Richard LeFever for their assistance and insight.

This work was made possible by funding from the U.S. Bureau of Reclamation, contract number 08FC602281, and the North Dakota Water Resources Research Institute.

I would like to thank Allen Schlag from the USBR for his guidance and assistance in obtaining sediment cores, Hanying Xu, director of UND'S Environmental Analytical Research Laboratory, for his knowledge and guidance throughout the analytical work, as well as Ryan Salinas Klapperich and Bijesh Maharjan for their guidance and encouragement.

I would like to thank my parents, Kent and Donna Christenson, for their love, support, and for always believing in me.

ABSTRACT

Denitrification, the microbial reduction of nitrate (NO_3^-) in groundwater, has three requirements: limited oxygen, bacteria capable of mediating the reaction, and electron donors for the bacteria to use in the redox reactions. The critical factor for aquifer denitrification is the concentrations of electron donors. Without an adequate supply of electron donors, bacteria cannot reduce concentrations of either oxygen or NO_3^-.

Artificial drainage within agricultural areas may allow contaminants to bypass, or increase conveyance through, reduced areas in which denitrification is likely to occur. This contributes to elevated NO_3^- yields as it is discharged directly into surface water. Depending on site geology, however, bacterial biofilms capable of NO_3^- reduction may cultivate within the tile drainage. This study aims to quantify and compare the potential for denitrification, as well as denitrification rates, within tile drainage and aquifer sediments at the Best Management Practices (BMP) site, within the Oakes Irrigation Test Area (OITA) near Oakes, North Dakota.

For the aquifer sediment study, sediment samples (n=43) were collected from 10 locations at the BMP site. All samples were analyzed for the following potential electron donors: organic carbon, ferrous iron, manganese, and inorganic sulfide. A subset of samples was analyzed for organic sulfur, but all were below detection limits (<0.01%). Samples were also analyzed for texture and color. For the subsurface

drainage study, a nutrient tracer test was conducted within a drain tile transect at the BMP site. Sediment samples (n=6) from the gravel pack surrounding the tile drains were analyzed in the same manner as the aquifer sediments.

The major finding was that the biofilm accumulation within the gravel pack surrounding the tile drains contains adequate electron donor concentrations. However, when compared with denitrification rates occurring in the aquifer sediments, the tracer test in the drain tile produced no observable denitrification. Secondary findings indicated that electron donors are correlated with one another and electron donor concentrations are inversely correlated with grain size in the aquifer sediments.

CHAPTER I

INTRODUCTION

The use of drain tiles for subsurface drainage has several advantages, including increased cropped acreage (Pavelis 1987), earlier planting seasons, increased crop yields (Eidman 1997), and decreased compaction of soil (Spaling and Smit 1995). Subsurface drainage may also reduce the use of and need for pesticides and fungicides by improving crop quality, thereby reducing the susceptibility of a crop to pests (Fraser and Fleming 2001). Drain tiles may also have disadvantages, such as increased peak flows during storm events (Robinson and Rycroft 1999), increasing nutrient concentrations in agricultural runoff (Downing et al. 1999) and they may become obstructed, resulting in reduced hydraulic efficiency. Obstructions can include silt deposits, roots, or sludge deposits and biofilms associated with bacterial activity (Ford 2005). Obstructions associated with bacterial activity involve the oxidation-reduction ("redox") cycling of sulfur (S), iron (Fe), and manganese (Mn) (Ford 2005) with oxygen in the drain tile. However, NO_3^-, like oxygen, is also a strong oxidant and it may be denitrified with these same elements (Korom 1992). Denitrifying bacteria have been confirmed in drain tiles (Ivarson and Sojak 1978, Knighton 1997) and biological clogging of drainage systems has improved water quality in situations involving extended retention time (Rowe and VanGulck 2004). Some investigators have speculated that denitrification may be occurring in the tile drain system in the Oakes Irrigation Test Area (OITA) (Knighton 1997, Casey et al. 2002, Derby et al. 2009,

Sawatsky 2009). Significant denitrification has also been known to occur in North Dakota aquifers (Korom et al. 2005, Korom et al. 2012). In this paper it is hypothesized that within the saturated zone, substantially more of the NO_3^- reduction in the OITA is occurring within the aquifer sediments at the site, rather than within the drain tiles. The aquifer sediments within the saturated zone of the OITA, not the drain tiles, are able to reduce NO_3^- at a rate which could be beneficial to water quality.

Agricultural Tile Drainage

Since the first recorded installation of drain tiles in 1835, the reclamation of land by subsurface drainage has transformed the American landscape (Framji and Mahajan 1969). Today, it is estimated that within the Mississippi basin alone, drainage pipes lie in the subsurface of an estimated 40-70 million acres (Hey 2001). The use of subsurface drainage continues to grow in the Midwest and has converted up to 30% of poorly drained wetlands to agricultural areas (Pavelis 1987). The recent wet cycle within the Red River Valley basin of North Dakota has caused tile-drainage to be installed within the region at a rapid pace (Figure 1). One drain tile installer within the region has reported installing more than 20 million feet of tile in the Red River Valley since 2005 (Nodak Electric 2011).

Overall, subsurface drainage remains a major pathway for nutrient (N and P) loss to surface waters (Blann et al. 2009). Subsurface drainage delivers nutrients to surface water via different pathways, and at different magnitudes. Enrichment of surface waters with nutrients is common in regions where intensive agriculture is practiced; the greatest riverine NO_3^- fluxes are observed from basins draining extensively drained agricultural regions (McIsaac and Hu 2004).

The eutrophication of downstream water bodies may be attributed to the leaching of NO_3^- and P out of the soil through subsurface drains (Dinnes et al. 2002). As subsurface drainage reclaims more land for agricultural production, it also creates environmental hazards on a global scale.

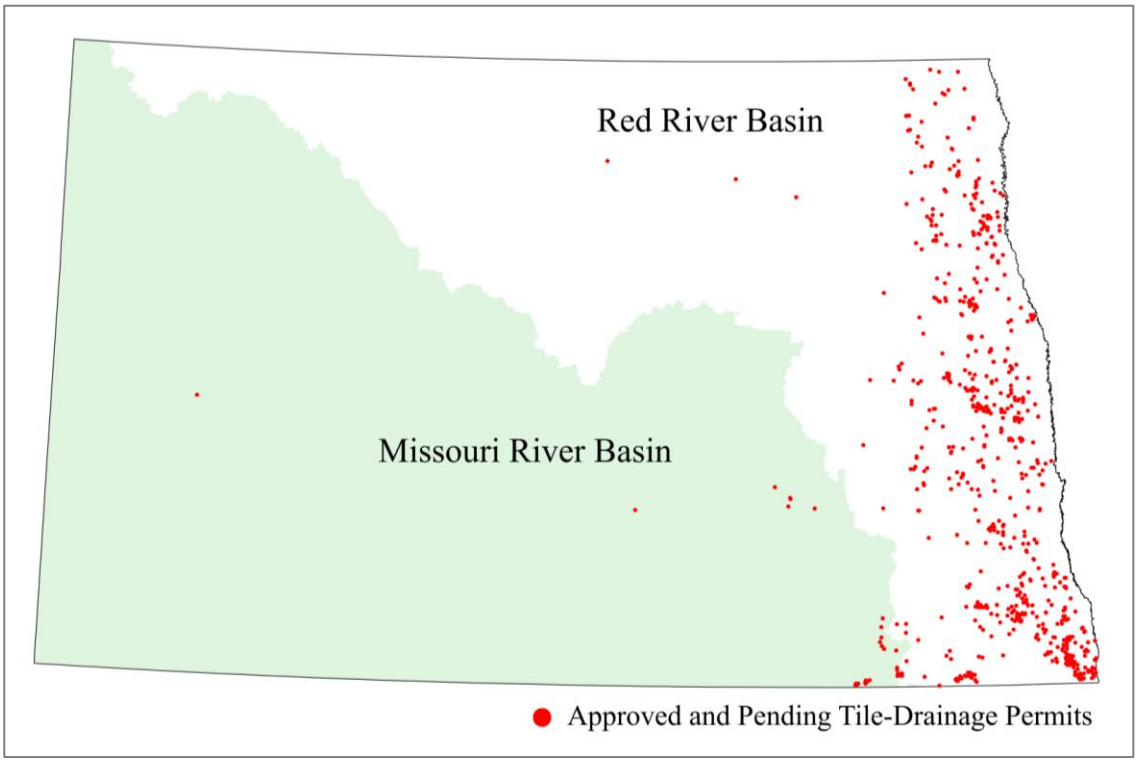

Figure 1. State-wide distribution of approved and pending tile-drainage permits (ND State Water Commission database, December, 2012).

Tile drains skim the NO_3^- from the surface of the aquifer and release it to nearby surface water. It is estimated that the principal contributor of nitrogen inputs to the Gulf of Mexico and the North Atlantic Ocean are agricultural in origin (Randall and Mulla 2001, Howarth et al. 1996). Increased NO_3^- loading in the Mississippi has been directly linked to the spread and increased severity of hypoxia within the Gulf of Mexico (Rabalais et al. 1996). Subsurface drains bypass the reduced zones where denitrification

is most likely to occur, contributing to higher NO_3^- yields as they discharge directly to surface water (Dinnes et al. 2002).

In some geologic environments, subsurface drainage may be beneficial to water quality. Draining soils increases their capacity to store moisture, which can reduce surface runoff volumes in certain situations. In comparison with surficial agricultural drainage, decreased surface runoff associated with drain tiles can improve water quality by reducing soil, chemical, and nutrient losses from a field (Fraser and Fleming 2001). Drain tiles have the potential to decrease pesticide loads by orders of magnitude; and phosphorus losses, which are generally associated with erosion, may be reduced (Gilliam et al. 1999, Ayars and Tanji 1999).

In agricultural soils, a high water table can have numerous negative impacts on crops. By removing excess water from the soil and lowering the water table, drain tiles enhance crop yields by allowing proper root-zone aeration and facilitating root proliferation, function, and metabolism (Fraser and Fleming 2001). Hydraulic efficiency in drain tiles is commonly reduced by mineral deposits, silt deposition and roots from nearby vegetation (Grass 1976). Biological clogging from bacteria may also affect hydraulic efficiency in drain tiles. The most prevalent and problematic form of biofilm accumulation is iron ochre, but biofilms may also be composed of manganese deposits, sulfur slimes, and iron-sulfides (Ford 2005).

Remediation of NO_3^- is effectively completed through the process of denitrification. This naturally-occurring process reduces NO_3^- to non-reactive nitrogen gas (Korom 1992). Denitrification requires the following: the availability of electron donors, an anaerobic environment, and the presence of nitrogen digesting bacteria

(Korom 1992, Starr and Gillham 1993). The availability of suitable electron donors within aquifer sediments has been shown to be the controlling factor in this reaction (Korom 1992 and references therein). According to Korom (1992), the most common electron donors are organic carbon, sulfide (typically as pyrite, FeS_2), and ferrous iron minerals, with manganese also possibly contributing. The same species are also cycled in drain tiles and may form biofilms or deposits that reduce hydraulic efficiency in drain tiles (Ford 2005).

Research has suggested that biofilms may be responsible for denitrification within subsurface lines in eastern North Dakota (Casey et al. 2002, Derby et al. 2009, Sawatzky 2009). As noted above, subsurface drainage tiles clogged with biofilm accumulation are potentially capable of the natural attenuation of NO_3^- by denitrification. Species of bacteria capable of denitrification, *Arthrobacter* spp. and *Brevibacter* spp., have been found within biofilm samples taken from subsurface drain tiles (Knighton 1997).

Samples of tile drain discharge from the Oakes Best Management Practices (BMP) research field have shown significantly lower NO_3^- concentrations than the nearby surrounding groundwater. These samples suggest that denitrification may be occurring via the manganese biofilm within the tile drains (Sawatzky 2009). On the other hand, Korom et al. (2005, 2012) showed that significant denitrification occurs by electron donors in aquifer sediments in North Dakota. My hypothesis is that more denitrification at the BMP site is occurring through the consumption of electron donors present within the aquifer sediments at the site, rather than through denitrification occurring within the tile drain system.

CHAPTER II

SITE DESCRIPTION AND GEOLOGY

The BMP site (Figures 2, 3, and 4) is a 64-ha agricultural field in the NW1/4, Sec. 29, T.130N, R.59W, Dickey County, ND, containing two transects of buried subsurface agricultural drainage. The primary objective for the BMP field site was to develop methods of monitoring leachate losses under irrigated crops (Derby et al. 1997). The BMP site is within a larger site, the OITA, which was constructed by the United States Bureau of Reclamation (USBR) in the 1980s to investigate feasibility of irrigation and artificial recharge in southeastern North Dakota from diverted James River water (Frietag and Esser 1986).

There are two lines of drain tiles that run from the south end of the BMP site to the north (Figure 4) where they intersect a drainage canal, which flows into the nearby James River. The drains at the site consist of corrugated plastic pipe, 6-inches (15 cm) or 8-inches (20 cm) in diameter, and buried approximately 8 feet (2.4 m) below the surface at the site. The BMP site tile drainage system differs from most current designs, in that the drainage is deeper and more widely spaced, six to eight feet (1.9 to 2.5 m) deep and 1,200 feet (366 m) apart. As a comparison, tile drain depths are generally three to four feet (1 to 1.2 m) deep and 40 to 100 feet (12 to 30 m) wide (Schuh 2008). Surrounding the tile drains is a 12-inch (30 cm) gravel envelope, with gravel brought in from off-site. A number of monitoring wells and field lysimeters (Derby and Knighton 2001) are installed in parallel east to west transects across the site. Details of the

instrumentation can be found in Derby and Knighton (2001), Derby et al. (1998), and Casey et al. (2002).

At the BMP site, a variety of clay, sand, silt, and gravel deposits cover the present surface. These sediments, the Oahe Formation, were deposited in environments including river, pond, wind-blown, and mass-movement (Bluemle 1979a).

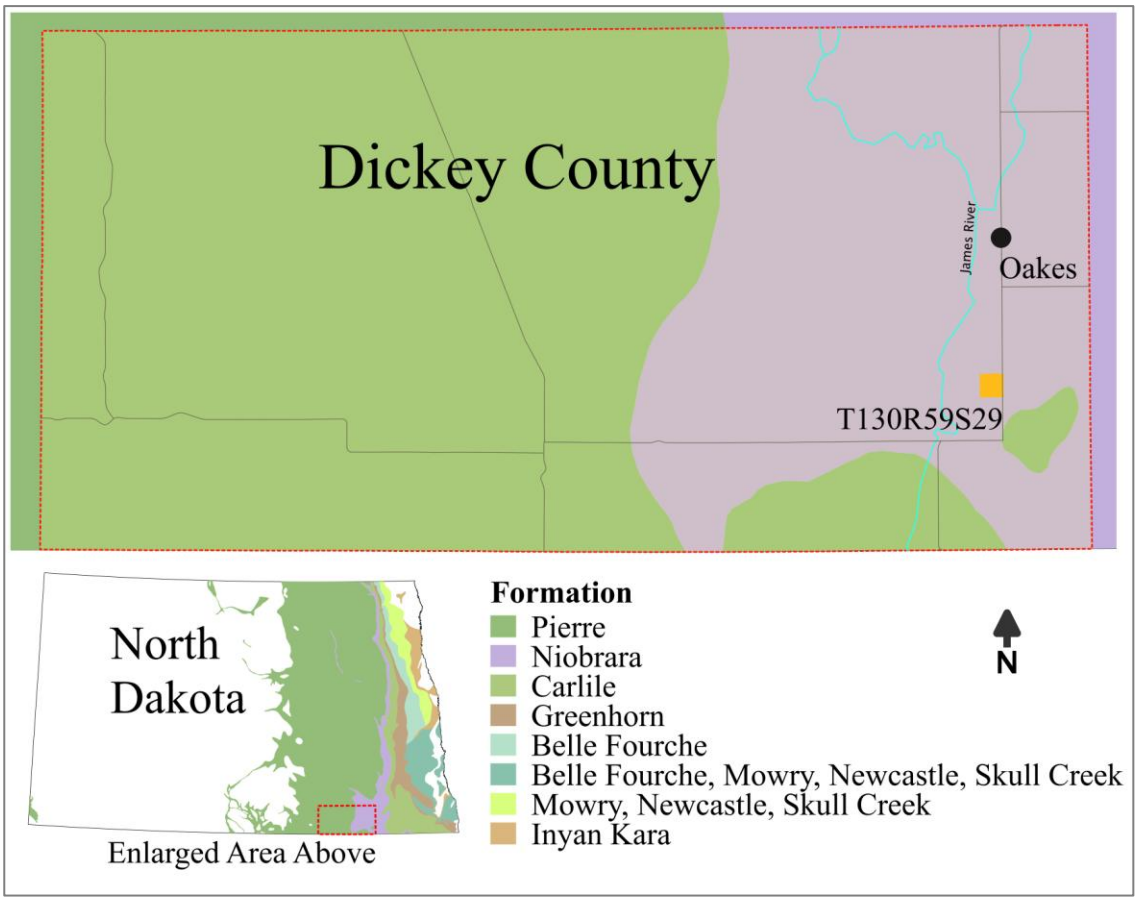

Figure 2. Underlying Bedrock near the Oakes Irrigation Test Area (OITA) (created using data from NDGIS Hub).

Several glacier advances and retreats likely scoured the underlying Niobrara and nearby Pierre formations to derive the facies of the Coleharbor. Till samples from the Coleharbor at various depths exhibit an average of 36% shale composition by weight (Bluemle 1979a).

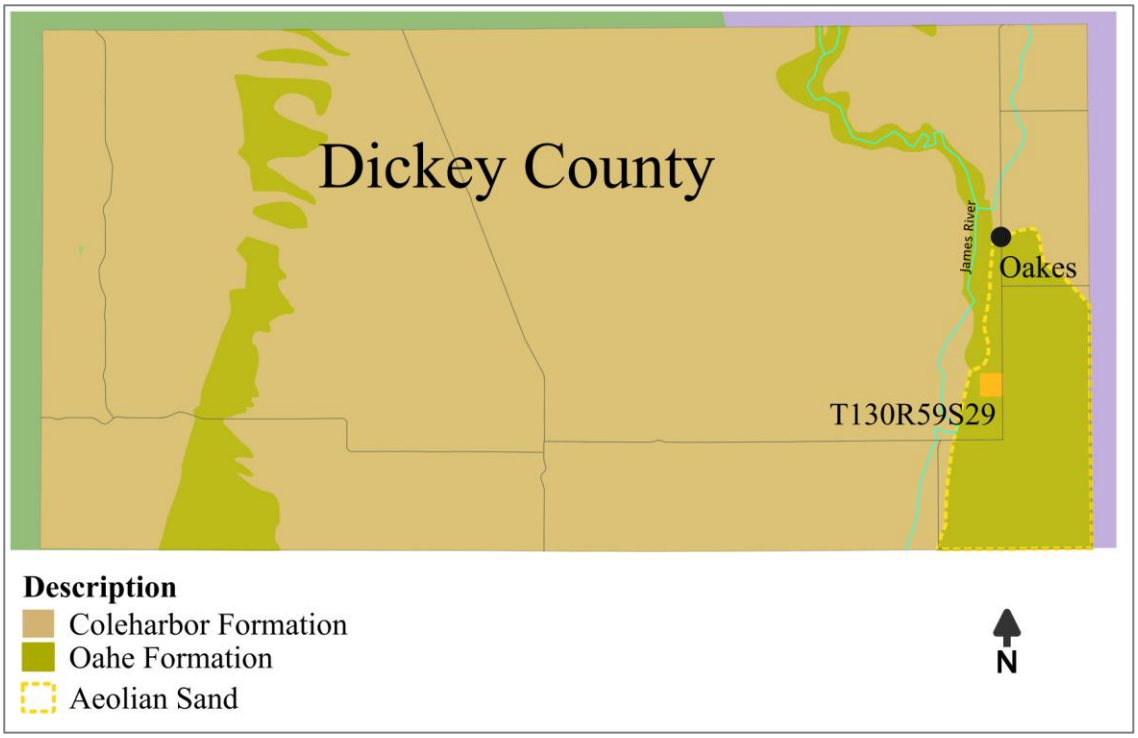

Figure 3. Map of surficial geology of Dickey County, ND (created using data from NDGIS Hub)

The Coleharbor Group overlies the Cretaceous Pierre Formation shale, with the exception of the eastern part of Dickey County where the Cretaceous Niobrara Formation is the underlying calcareous shale formation (Figure 2 and Table 1). The shales of the Pierre Formation are commonly found exposed on the east side of the Missouri Escarpment, where Coleharbor Group sediments become thin. In a similar study involving electron donor potential, the Niobrara Formation was shown to have over twice the amount of available electron donors as the Pierre Formation in east-central North Dakota (Klapperich 2008).

The BMP site sits atop the unconfined Oakes aquifer, underlying an area of about 93 mi^2 (240 km^2), with the James River creating a flow boundary along the western edge. The aquifer was the result of a two separate stages of deposition. The early, lower aquifer materials were deposited as valley fill. These deposits consist of

fine to coarse sand and gravel with interbedded silt and clay deposits. After the valley became blocked in the south, glacial Lake Dakota was formed and covered an area from South Dakota to 3 miles (5 km) north of Oakes. During the Lake Dakota stage, the deposited aquifer materials were of deltaic and lacustrine origins, with fine to medium sand and silt, and silt and silty clay.

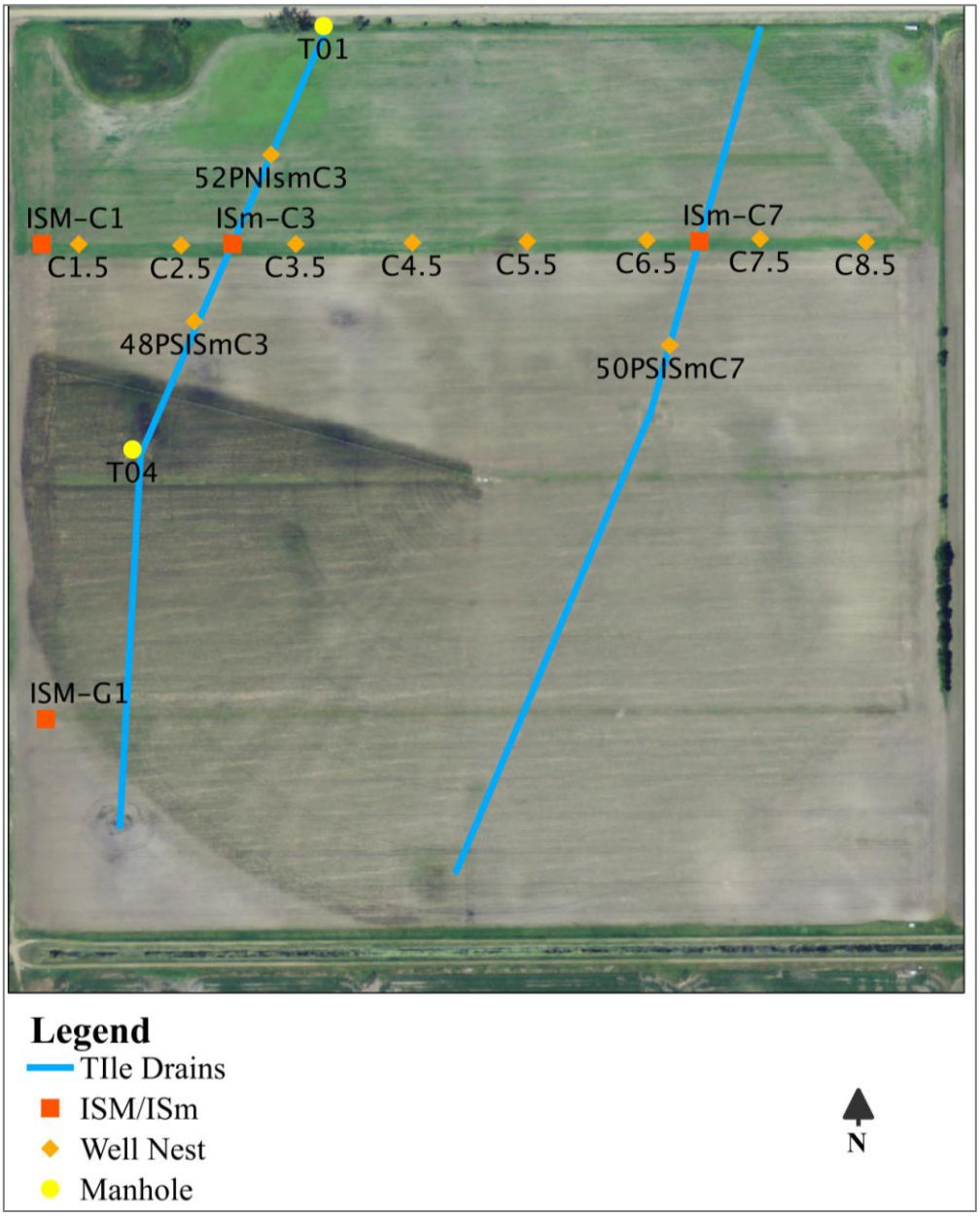

Figure 4. Overview of BMP test site showing sediment sample locations, ISM/ISm locations, and tile drain transects.

These deposits form the majority of the present land surface in the region (Armstrong 1980). Oakes sits near the stratified sand and gravel deposits similar to a deltaic complex. These delta deposits are composed of quartz, shale, lignite, Canadian shield silicate, and carbonate sediments (Bluemle 1979a). Considering the proximity of the Oakes aquifer, the black noncalcareous shales within the delta deposits are likely derived from the Niobrara shale.

Table 1

Simplified Stratigraphic Column of Dickey County, Showing Formations of Interest (adapted from Bluemle 1979a)

AGE	UNIT NAME	DESCRIPTION	THICKNESS (m)
Quaternary	Oahe (Holocene)	Sand, silt, and clay	?
	Coleharbor (Pleistocene)	Till, sand, gravel, silt, and clay	0 – 183
Tertiary			Absent
Cretaceous	Pierre Formation	Shale	366 – 549
	Niobrara Formation	Calcareous shale	

CHAPTER III

MATERIALS AND METHODS

The overall objective of this research is to quantify, locate, and understand the occurrence of denitrification within an artificially drained agricultural site. It was determined that three possible settings existed within the OITA that may be capable of denitrification: the aquifer sediments, the tile-drain gravel pack, and within the tile drain itself. In order to determine and compare the denitrification potential of these three sources, a two-part study was created. Analysis of aquifer sediments for electron donors, and the measurement of denitrification rates within the sediments and tile drain gravel pack comprise the first part of the study. For the second part of the study, a pair of tracer tests were conducted within a transect of drain tile.

Aquifer Denitrification Research

Subsurface sediment samples were collected in September of 2008 by coring the aquifer sediments at the study site. Eighteen potential sample locations were identified based on previous well logs. Hydraulic soil sampling equipment from the USBR was used to collect the samples. Several samples were collected from each site at varying intervals. Additional samples were collected from the tile drain gravel pack during June and July of 2009. A total of 15 sites yielded 49 samples, the locations of which are marked on Figure 4. Samples were collected in acrylic core sleeves (ID = 2.54 cm, OD = 2.82 cm), labeled, and capped at both ends before being placed in

coolers and transported to the University of North Dakota. The samples were later placed in glass jars, labeled, and frozen until needed for analysis.

The samples were analyzed for texture, inorganic carbon (IC) and organic carbon (OC) content, inorganic sulfide (IS) and organic sulfide (OS) contents, ferrous iron [Fe(II)] content, manganese (Mn) contents, and Munsell color. Only the sediments smaller than gravel (<2.0mm) were analyzed for electron donor contents and IC. Prior to any chemical analysis, each sample was first oven dried overnight at 103°C and ground into a fine powder.

OC was determined by a high temperature combustion method (Churcher and Dickout, 1986). IS was determined by chromium reduction modified slightly by using larger amounts of reagents (Canfield et al. 1986). Fe(II) and Mn were measured through wet chemical extraction (Klapperich 2008) by adapting methods used by Kennedy et al. (1999). The results of total Fe(II) combined the Fe(II) recovered by the wet chemical extraction method and the Fe(II) corresponding to IS, which is assumed to be primarily from pyrite (FeS_2). From the sediment samples, 14 were randomly selected for analysis of OS in a Leco SC-432 DR Sulfur Analyzer. All chemical analyses were completed at UND's Environmental Analytical Research Laboratory (EARL). Duplicate analyses were performed as quality control for the entire OC analyses, and less frequently for other analytical techniques. Appendix A includes detailed methodologies for all analyses.

Statistical analysis was carried out on the electron donor data from the 49 aquifer sediment sample locations. The normality of the individual populations was tested prior to the comparison of electron donor distribution. This was accomplished

via the Shapiro and Wilk "W-test" (Gilbert 1987). Each donor was tested for both the lognormal transformed and non-transformed populations. Based on the results from the "W-test" (Appendix B) the non-parametric Spearman Rho test (Conover 1971), which does not assume an underlying distribution, was employed for statistical analysis.

Correlations between the different donors and different sediment facies were tested. The data for the tile drain gravel pack samples were not included in the sediment correlation, as no textural analysis was performed on those samples. The one-tailed version of the Spearman Rho test using critical values corresponding to $\alpha = 0.10$, $\alpha = 0.05$, and $\alpha = 0.01$ was used to determine if positive or negative correlations existed.

In-situ denitrification rates for the aquifer sediments at the OITA were measured using a pair of stainless steel chambers driven into the aquifer sediments, referred to as "in-situ mesocosms" (ISMs). The ISM developed by Schlag (1999) is a larger version, with an aquifer volume of 186 L, of the in-situ microcosms (ISm) used for Gillham et al. (1990) and Bates and Spalding (1998). The ISM, a stainless steel cylindrical chamber measuring 0.39 m in diameter by 1.5 m long, permits sizeable water quality samples (~1L) to be obtained regularly over long periods (>2 years). Since their first use in the Elk Valley Aquifer in northeastern North Dakota, ISMs have successfully monitored the chemical evolution of groundwater at several sites (Korom et al. 2005, Korom et al. 2012).

Suitable ISM locations were determined based on cross sectional maps of the aquifer sediments provided by the USBR. Locations were selected with the goal of measuring the denitrification rates in distinctly different aquifer sediment textures. In-situ denitrification rates were measured using stainless steel chambers at four sites.

Two sites employed ISMs, ISM-C1 and ISM-G1 (Figure 4), which enclosed coarse aquifer materials and fine-grained sands, respectively. For the remaining sites, a much smaller chamber was used, an in-situ microcosm (ISm) with a sediment volume of 3.2 L. The smaller chamber size of the ISm allowed for a water sample from within the gravel pack surrounding the tile drains.

ISM-G1 was installed 4.5-6 meters below the land surface, in fine-grained aquifer sediments near the G1 well nest (Figure 4). ISM-C1 was installed 4-5.6 meters below the land surface, in coarse-grained aquifer sediments near the C1 well nest (Figure 4). Two tracer tests were performed in each ISM to determine in situ denitrification rates. The first gravel pack ISm, ISm-C3, was installed 1.5-2 meters below the land surface, within the tile drain gravel pack next to well nest C3 (Figure 4). The ISm was later reinstalled at the same depth in the gravel pack near well nest C7 (Figure 4). Gravel for the envelope around the tile drains was imported from off-site, denitrification occurring within the envelopes would likely be from the development of manganese bacteria growth within the gravel pack pore spaces.

For the sampling of the ISMs and ISms, Groundwater was pumped from the site into a reservoir, amended with NO_3^- and Br^-, and then siphoned back into sampling devices. The dilution of amended water with native groundwater was measured with Br^- tracer. Any loss of NO_3^- beyond what is explained by the dilution of Br^- was attributed to denitrification. Korom et al. (2005) described in detail ISM installation, amendment, and sampling methodology.

Tile Drain Denitrification Research

On the 3rd and 4th of June 2008, two tracer tests were performed within a transect of drain-tile at the Oakes BMP site. The tests were conducted for the purpose of investigating the possibility of NO_3^-, PO_4^{3-} and NH_4^+ removal and/or uptake by drain tile biomass. The tracer tests were conducted with the 20-cm (8-inch) diameter tile-drain between manhole T04 and manhole T01 (Figure 4).

The first tracer test, performed on June 3, 2008, involved the injection of NaCl into the drain at manhole T04. The purpose of this test was to establish a sampling schedule for the second tracer test based on the comparison of electrical conductivity (EC) versus time at the downstream manhole T01 (Table 16).

A total volume of 15 L of water was bailed from manhole T04 and transferred into a reservoir. The water in the reservoir was amended with 737 g of food grade NaCl, thoroughly mixed, and then injected directly into the drainage pipe at manhole T04 over two minutes. The EC was recorded within the drainage pipe at manhole T01 for approximately three hours.

The data from the first tracer test showed that the peak EC occurred approximately 100 minutes following the injection, with the beginning pulse arriving in 86 minutes and returning to near-background levels in 200 minutes. Based on this information, monitoring of the second tracer test would begin one hour subsequent to the injection and continued at regular intervals for nearly four hours following the injection.

The second tracer test was performed on June 4, 2008. A total volume of 10 L of water was bailed from manhole T04 and transferred into a reservoir. The water in the

reservoir was amended with reagents listed on Table 2. The amended water was injected directly into the drainage pipe at manhole T04 over the course of one minute.

Water samples were collected using an improvised sampling device within the drainpipe at Manhole T01. Following collection, the samples were passed through 0.45 μm disposable filters, then preserved and stored for analysis. Samples to be analyzed for NO_3^--N and Br^- were filtered directly into 60 mL plastic bottles. Samples to be analyzed for total phosphorus (TP) and NH_4^+-N were filtered directly into 250 mL plastic bottles containing 1 mL of concentrated H_2SO_4 for every 50 mL of sample.

Table 2

Reagents Added for 2nd Tile Drain Tracer Test

Reagent	Constituent Monitored	Constituent Amount Added (g)
$NaNO_3$	NO_3^--N	39.00
NaBr	Br^-	32.50
$NaH_2PO_4 \cdot H_20$	Total P (TP)	8.03
NH_4Cl	NH_4^+-N	7.80
Volume:	10 L	
Rate of Injection:	10 L/min	
Duration of Test:	229 min	

Analyses were performed at the University of North Dakota's EARL. Br^- and NO_3^--N were analyzed with the use of a Dionex DX-120 Ion Chromatograph. TP was analyzed using HACH kit, method #8190. NH_4^+-N was analyzed as NH_3 using an Accument ion selective electrode. However, at the pH levels of the water in the tile drain, ammonium is the dominant species. To return the pH of acidified samples to neutral, NaOH was added as required during analysis of TP.

CHAPTER IV

RESULTS AND DISCUSSION

Aquifer Sediments

The textural analysis was modified based on the classification of grain sizes adopted from USGS (2003). All 49 samples were analyzed for gravel, sand (coarse, medium, and fine), silt, and clay contents. Figure 5 illustrates the weight percent of electron donors for each sediment texture classification including the gravel pack for comparison. Detailed results of the sediment texture analysis are reported in Appendix B.

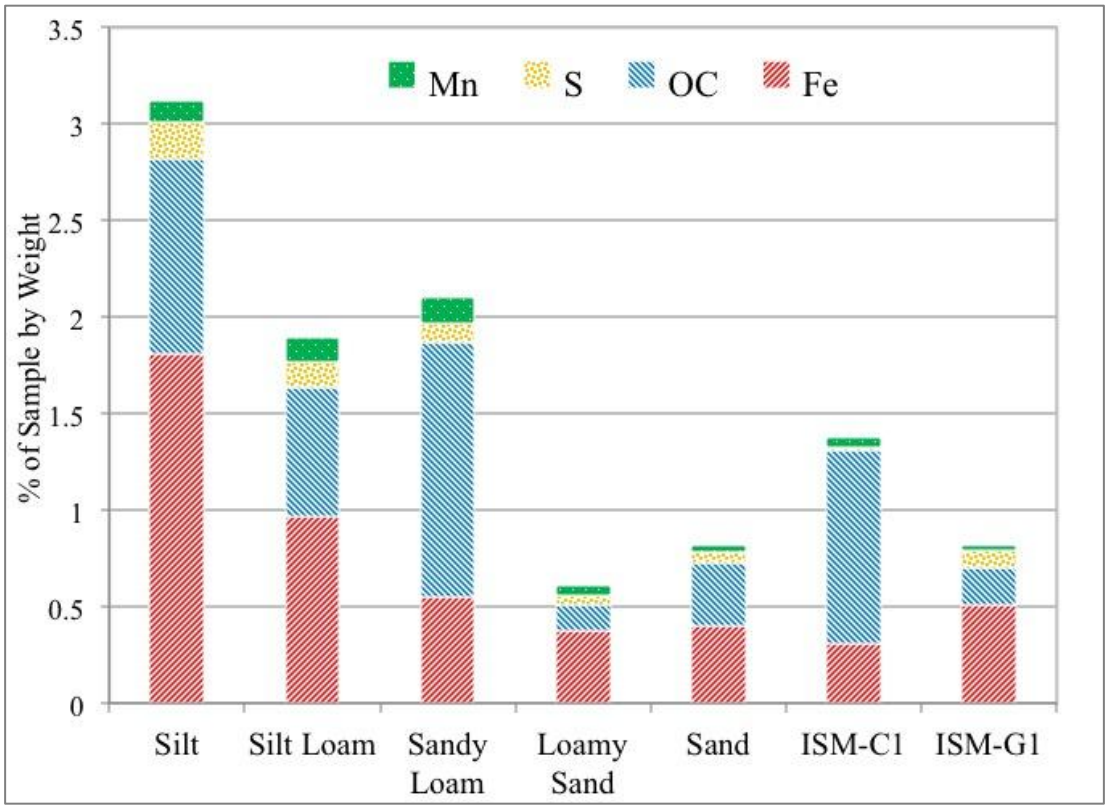

Figure 5. Weight percent of electron donors.

Table 3

Results of Each e^- donor Test. All Results are Reported by Weight %. Results for the Organic Donors Represent Values Adjusted for Pre-treatment (PT) Weights

Sample ID	Textural Classification	%S^-	OC (PT Eq) (%)	Mn (%)	Fe(II) (%)	Avg Pyrite Fe (%)	Total Fe(II) (%)
ISM-C1 A	Sandy Loam	0.007	0.087	0.299	0.090	0.006	0.096
ISM-C1 B	Loamy Sand	0.011	0.067	0.089	0.030	0.010	0.040
ISM-C1 C	Sand	0.024	0.104	0.012	0.327	0.021	0.348
ISM-C1 D	Sand	0.004	0.073	0.035	0.153	0.004	0.157
ISM-C1 E	Sand	0.009	1.664	0.098	0.302	0.008	0.310
ISM-C1 F	Sand	0.020	1.186	0.019	0.267	0.018	0.285
ISM-C1 G	Sand	0.032	0.150	0.021	0.300	0.029	0.329
ISM-C1 H	Silt Loam	0.014	0.557	0.112	1.591	0.012	1.603
C1.5 A	Loamy Sand	0.000	0.404	0.068	0.324	0.000	0.324
C1.5 B	Loamy Sand	0.102	0.312	0.041	0.455	0.091	0.546
C1.5 C	Sandy Loam	0.169	0.753	0.080	0.566	0.151	0.717
C1.5 D	Silt Loam	0.232	0.739	0.206	0.118	0.207	0.325
C2.5 A	Loamy Sand	0.003	0.067	0.047	0.118	0.003	0.121
C2.5 B	Loamy Sand	0.071	0.136	0.040	0.208	0.063	0.271
C2.5 C	Sandy Loam	0.103	4.410	0.065	0.445	0.092	0.537
C2.5 D	Sandy Loam	0.083	2.101	0.241	0.814	0.074	0.888
C2.5 E	Silt Loam	0.044	0.729	0.073	0.535	0.039	0.574
C3.5 A	Sand	0.013	0.180	0.002	0.422	0.012	0.434
C3.5 B	Sandy Loam	0.157	0.172	0.035	0.296	0.140	0.436
C3.5 C	Silt Loam	0.132	0.444	0.071	0.542	0.118	0.660
C3.5 D	Silt Loam	0.224	0.510	0.160	0.624	0.200	0.824
C4.5 A	Loamy Sand	0.003	0.020	0.115	0.030	0.003	0.033
C4.5 B	Loamy Sand	0.057	0.036	0.047	0.336	0.051	0.387
C4.5 C	Loamy Sand	0.099	0.096	0.118	0.533	0.088	0.621
C4.5 D	Sand	0.091	0.035	0.055	0.472	0.081	0.553
C5.5 A	Sand	0.015	0.023	0.100	0.177	0.013	0.190
C5.5 B	Loamy Sand	0.007	0.084	0.027	0.475	0.006	0.481
C5.5 C	Sandy Loam	0.076	0.357	0.034	0.561	0.068	0.629
C5.5 D	Sand	0.084	0.389	0.028	0.533	0.075	0.608
C5.5 E	Sand	0.119	0.727	0.004	0.534	0.106	0.640
C6.5 A	Sand	0.000	0.036	0.006	0.151	0.000	0.151
C6.5 B	Loamy Sand	0.107	0.091	0.003	0.485	0.096	0.581
C6.5 C	Loamy Sand	0.127	0.056	0.005	0.480	0.113	0.593
C6.5 D	Silt	0.187	1.012	0.110	1.640	0.167	1.807
C7.5 A	Loamy Sand	0.002	0.068	0.018	0.120	0.002	0.122
C7.5 B	Loamy Sand	0.021	0.361	0.052	0.398	0.019	0.417
C7.5 C	Sand	0.136	0.108	0.064	0.417	0.121	0.538
C7.5 D	Sand	0.149	0.169	0.051	0.508	0.133	0.641

Table 3 (continued)

Sample ID	Textural Classification	%S^-	OC (PT Eq) (%)	Mn (%)	Fe(II) (%)	Avg Pyrite Fe (%)	Total Fe(II) (%)
C8.5 A	Sand	0.001	0.133	0.024	0.177	0.001	0.178
C8.5 B	Sand	0.082	0.065	0.017	0.421	0.073	0.494
C8.5 C	Loamy Sand	0.126	0.106	0.053	0.501	0.112	0.613
ISM-G1 A	Sand	0.093	0.222	0.003	0.449	0.083	0.532
ISM-G1 B	Loamy Sand	0.000	0.166	0.045	0.484	0.000	0.484
ISm-C3GP	Gravel Pack	0.012	0.888	3.233	0.029	0.011	0.040
ISm-C3BGP	Gravel Pack	0.000	0.413	0.415	0.059	0.000	0.059
48PSISmC3	Gravel Pack	0.023	1.193	0.221	0.138	0.021	0.159
52PNISmC3	Gravel Pack	0.005	1.485	0.220	0.179	0.004	0.183
ISmC7GP	Gravel Pack	0.002	0.723	0.221	0.016	0.002	0.018
50PSISmC7	Gravel Pack	0.001	0.370	0.083	0.045	0.001	0.046

Organic Carbon

From 49 individual samples, 98 OC analyses were performed (Table 3). The highest OC concentrations were measured in silt with 1.01% by weight, and the lowest OC values were 0.02% by weight for loamy sand and sand. OC accounted for approximately 42% of the e^- donors available in the sampled material from the OITA. A few sandy-loam and sand samples contained anomalous percentages of OC. These were assumed to be buried paleosols, and remained included in the analysis. It is also a significant e^- donor within each sediment facies. Duplicates show fair reproducibility well below a percent difference of 25%. The complete OC results and calculations are reported in Appendix B.

Silt loam samples contained the highest amounts of organic carbon, ranging from 0.38% to 0.84% by weight. OC accounted for about 31% of the e^- donors available within the silt loam sediment facie samples. Loamy sand analyses showed an average OC concentration of 0.17% by weight, contributing to 27% of the e^- donors

available within that particular facies. The sand facies also showed significant OC contents, at 0.33% OC by weight, contributing to 40% for e^- donors available within the facies.

Inorganic/ Organic Sulfide

Overall, IS accounts for about 5% of the total electron donors present in the sediment samples. Values ranged from 0.003% in sand to 0.232% in silt loam. With pyrite noted as the most commonly occurring sulfide mineral, it was assumed that all of the IS measured in this test was in the form of pyrite (Schoonen 2004). IS was measured below the detection limit in eight of the samples, all of them texturally classified as sand or loamy sand.

Inorganic sulfide within the silt loam samples averaged about 0.14% by weight and account for about 7% of the e^- donors present within the silt loam (Figure 5). Within the loamy sand samples, IS averaged nearly 0.06% by weight and accounted for about 8.8% of the e^- donors present within the loamy sand samples. The sand samples also averaged 0.06% IS by weight accounting for nearly 10% of the e^- donors present within the sand samples. Pyrite recoveries for inorganic sulfur analysis were >95%. The complete results and calculations are shown in Appendix B.

Klapperich (2008) determined that a modified method of inorganic sulfide analysis could be used for organic sulfide (OS) analysis. Based on his methods, testing for IS was repeated on 14 samples. The entire set of 14 samples yielded OS results below detection. The duplicate analyses yielded organic sulfide results below detection. Therefore, OS as an electron donor was not considered further in the present study.

Klapperich (2008) noted that OS yielded the lowest values of e^- donors tested in his electron donor research within bedrock formations.

Ferrous Iron

Ferrous iron results are the product of two tests: the Fe(II) associated with pyrite as is measured by the Canfield method, and measured as non-pyritic Fe(II) by the modified Kennedy technique using wet chemical extraction. Ferrous iron follows the pattern of the other e^- donors within the facies, being low in sand and higher in silt loam. Ferrous iron is also a dominant e^- donor present in all the facies, averaging near 46% Fe(II) by weight of all samples included in this study. Of the 49 analyses, the highest value came from a silt sample with an average value of 1.81%. The lowest Fe(II) values, 0.03% and 0.02% were from loamy sand and gravel samples, respectively. The complete Fe(II) results and calculations are reported in Appendix B.

Ferrous iron was significantly more abundant in the silt loam facies than the other e^- donors. The overall Fe(II) average for the silt loam facies was 0.97% by weight. The loamy sand and sand facies showed nearly the same overall Fe(II) average with 0.38% and 0.40% concentrations by weight, respectively.

Manganese

A method similar to that used for Fe(II) was applied to determine manganese concentrations in the sediment facies. Rhodochrosite ($MnCO_3$) recovery produced an average manganese recovery of 85%. The complete manganese results and calculations are reported in Appendix B.

Overall, manganese accounted for approximately 6% of the total e^- donors present in all the samples. Values ranged from 0.002% to 0.299% within a sand and

sandy loam, respectively. The tile drain gravel pack contained significant amounts of manganese, averaging 0.74% by weight, likely due to the manganese biofilm accumulation associated with the tile drains. With the exception of the tile-drain gravel pack, the values for manganese also appear to follow the pattern of increasing e^- donor concentration with decreasing sediment size.

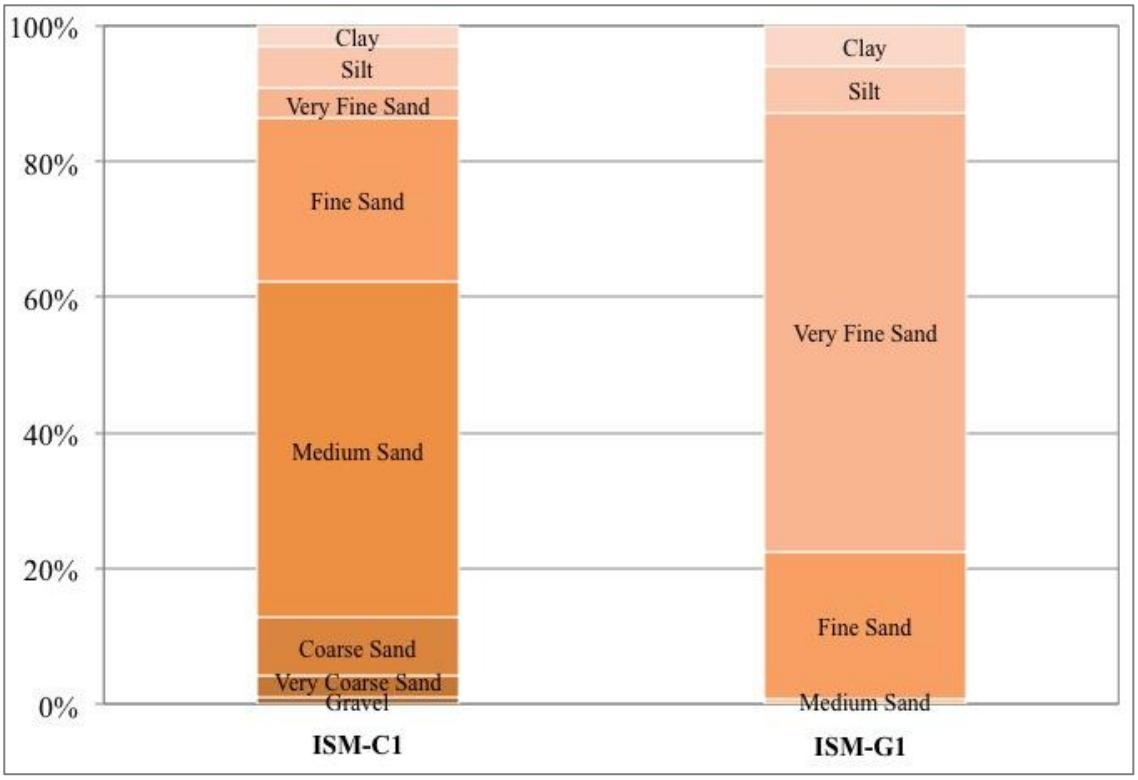

Figure 6. Chart showing textural analysis of ISM-C1 and ISM-G1.

Comparison of electron donors by weight percent with another site of denitrification study within eastern North Dakota shows the OITA having higher OC percentages within the three finer-grained sediment textures. The sandy loam, silt loam, and silt present at the OITA have an average range of 0.665% to 1.319% OC by weight, whereas sediments from the Elk Valley Aquifer in eastern North Dakota had a maximum OC content of 0.43% (Korom et al. 2005). Both of these sites contain

relatively high OC when compared with the Karlsruhe site, having 0.017% OC (Korom et al. 2012).

Statistical Correlations

The results from the Shapiro and Wilk "W-test" (Appendix B) showed that the electron donors could not be considered to be normally distributed, regardless of log transformation or not. The results of the Spearman Rho test, presented in Table 4, indicated that a positive correlation at a significance level of $\alpha = 0.01$ was found between inorganic sulfide and ferrous iron, as well as organic carbon and manganese. At a significance level of $\alpha = 0.10$, positive correlations exist between inorganic sulfide and organic carbon, organic carbon and ferrous iron. Organic carbon and manganese were positively correlated with silt at $\alpha = 0.01$, whereas ferrous iron was correlated with silt at $\alpha = 0.05$. Once again, if the significance level is expanded to $\alpha = 0.10$, inorganic sulfide is also positively correlated with silt. All of the electron donors showed a negative correlation with sand textures. Manganese was positively correlated to both silt and clay. Organic carbon was positively correlated with both gravel and silt. The sediment textures failed to show a positive correlation, with gravel and sand negatively correlated as well as sand and silt.

Maharjan (2009) found similar correlations between electron donors and sediment texture at a study site within eastern Iowa. The eastern Iowa site showed a higher correlation of electron donors with clay than silt, whereas the OITA electron donors were correlated with silt. This difference is likely due to the sandy nature of the aquifer at the OITA and its lack of clay textures. Also similar to the eastern Iowa site, the electron donors IS and Fe at the OITA are positively correlated to one another at α

= 0.01. If we increase the significance level to α = 0.10; IC, Fe, and OC are all positively correlated to one another. Manganese as an electron donor was not studied at the eastern Iowa site.

Table 4

Results of Spearman's Rho Test

Spearman Rho for positive correlation

Ho: There is not a positive correlation of the two donors' average values

	IS	OC	Fe	Mn	Gravel	Sand	Silt	Clay
IS	X	0.187*	0.748	-0.071	0.178	-0.298	0.206*	0.222*
OC		X	0.234*	0.398	0.405	-0.463	0.424	0.104
Fe			X	-0.160	0.108	-0.390	0.281	0.212*
Mn				X	0.199*	-0.463	0.456	0.295
Gravel					X	-0.269	0.064	0.097
Sand						X	-0.912	-0.108
Silt							X	0.011
Clay								X

Positively correlated at 0.05 α

Positively correlated at 0.01 α

Negatively correlated at 0.05 α

Negatively correlated at 0.01 α

*. Indicates correlation significant at 0.10 α

ISM/ISm Results

The first ISM tracer test (TT1) lasted 112 days, starting August 13, 2008 and ending December 2, 2008, the first ISm tracer test was initiated at the same time. The second ISM tracer test (TT2) lasted 129 days, starting June 2, 2009 and ending October 10, 2009. The second ISm tracer test began on day 50, or July 3, 2009, of the second ISM tracer test. During both periods the general aqueous chemistry species were monitored, which included products and reactants associated with denitrification

The relative change of the dilution-tracing Br^- is of importance to our study of denitrification in the aquifer sediments. Tracking Br^- in the ISM/ISm's permits the evaluation for NO_3^--N removal via dilution or through denitrification. The normalized concentrations of these anions are displayed in Figure 6 for the tracer tests at the four Oakes sites. This shows the concentration trends and relative changes compared to dilution.

During the first tracer test, the NO_3^--N concentration in the ISM-G1 began at 76.2 mg/L and was reduced to 6.63 mg/L throughout the 112 day test. The Br^- concentration in ISM-G1 began at 44.4 mg/L and remained at 95.1% of the amended concentration for the course of the experiment. When corrected for dilution, the denitrification rate in ISM-G1 was 0.59 mg/L/day for TT1. In contrast, during the first tracer test for ISM-C1 the Br^- began at 40.7 mg/L and diluted to 18.2 mg/L, retaining 44.7% of its initial concentration. When TT1 for ISM-C1 is corrected for dilution, the denitrification rate becomes 0.06 mg/L/day. It appears as though ISm-C3 also exhibited a similar dilution as shown by Br^- concentrations, with 51.0% of the amended concentration remaining. When corrected for dilution, the denitrification rate within ISm-C3 was 0.11 mg/L/day. Figure 7 illustrates the dilution corrected Br^- and NO_3^--N zero order denitrification rates.

During the second tracer test (TT2), the NO_3^--N concentration in the ISM-G1, experienced a less significant loss (Figure 7) beginning at 72.5 mg/L and dropping to 30.5 mg/L throughout the 129 day test. The Br^- concentration in ISM-G1 began at 43.4 mg/L and remained within 91.3% of the initial concentration. When corrected for dilution, TT2 for ISM-G1 indicates a denitrification rate of 0.28 mg/L/day. Once

again, during the second tracer test for ISM-C1 the Br^- shows evidence of tracer test dilution, with Br^- concluding TT2 with 46.7% of the initial concentration.

The denitrification rate for TT2 within ISM-C1 is comparable to the first at 0.03 mg/L/day. During the course of TT2, ISm-C7 Br^- concentrations remained within 93.1% of their initial concentration. When corrected for dilution, ISm-C7 indicated a denitrification rate of 0.30 mg/L/day; however, fit of the data to zero-order denitrification is not as good as for the other tracer tests (Figure 8). The ISm-C7 tracer test began 48 days after the start of the second tests in ISM-G1 and ISM-C1.

Denitrification rates for the tracer tests conducted at the OITA are expressed as zero-order denitrification reactions. Zero-order reactions are generally the standard for the majority of published aquifer denitrification rates (Korom 1992, Green et al. 2008, Korom 2012). Compared to another eastern North Dakota ISM site, a site whose published zero-order denitrification rate was amongst the highest recorded in the literature, the ISM-G1 rate is 1.9 times faster at 0.59 mg/L/day (Korom et al. 2005, Green et al. 2008).

Comparison of the rate found within ISM-C1to the same site shows ISM-C1 to be 4.9 times slower at 0.06 mg/L/day. The zero-order denitrification rate for ISM-C1 is comparable to those rates found within the Karlsruhe aquifer of north-central North Dakota. The zero-order denitrification rates found within the ISms placed in the tile-drain gravel pack at the OITA, an average of 0.20 mg/L/day, were similar to the first tracer test in the Elk Valley Aquifer (Korom et al. 2005).

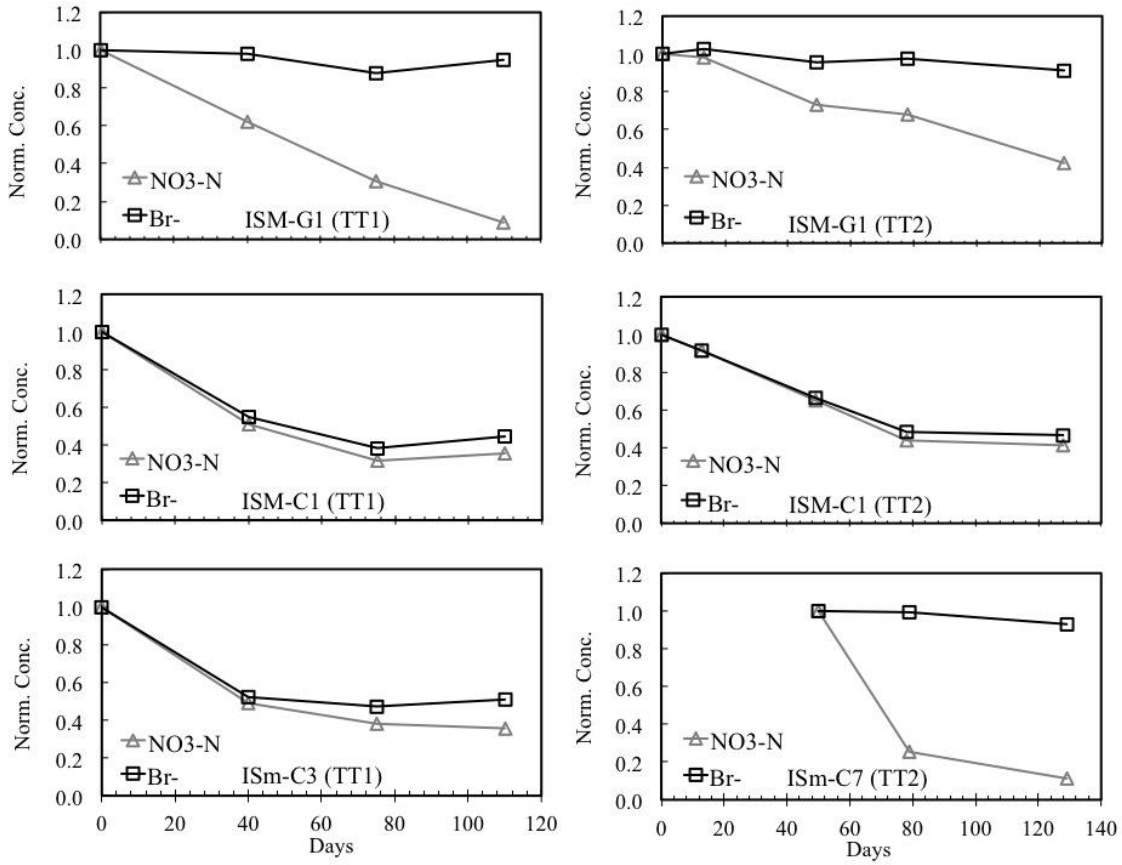

Figure 7. Important anions from ISM/ISm tracer tests.

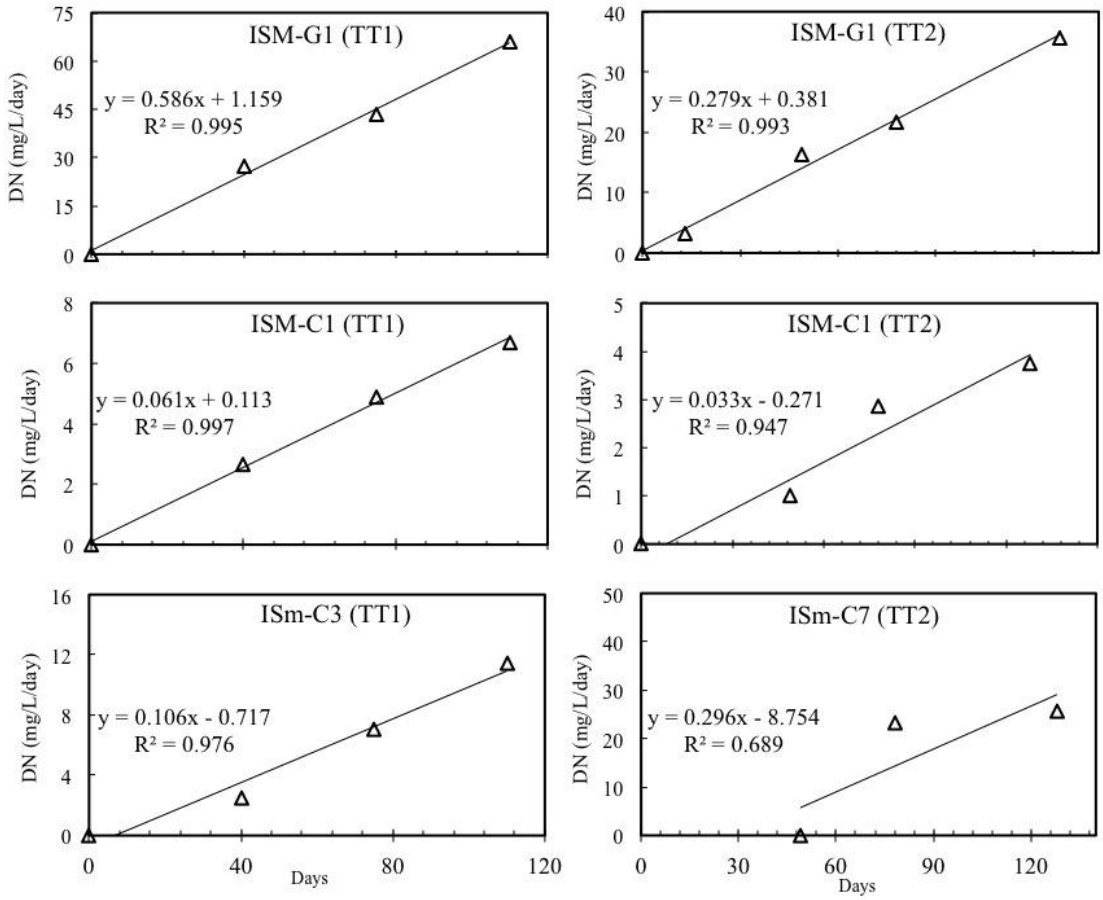

Figure 8. Zero-order denitrification rates observed from ISM/ISm tracer tests.

Drain Tile Tracer Test

For the drain tile test conducted on June 4, 2008, the concentrations for each analyte were plotted versus time (Figure 8). The area under each curve was calculated and background concentrations were removed. Anions, NO_3^--N and Br^-, were analyzed twice with two injections per analysis. The concentration of each analyte was then plotted with the concentration of bromide over time and the ratio of the two areas calculated (Table 4). The ratios of bromide to each analyte for the amended water and the ratios obtained from the tracer analysis are presented in Figure 9.

The amended water for the tracer test had a Br^- to NH_4^+-N ratio of 1: 0.24, and the results from the analysis yielded a ratio of 1: 0.30. This increase indicates a

production of NH_4^+. Being the only cation measured during the tracer test, the increased Na^+ in the amended water was likely exchanged for NH_4^+ on cation exchange sites on minerals and organic matter in the biomass in the tile drain. Without the analysis of all major cations, this hypothesis cannot be further evaluated. The amended water for the tracer test had a Br^- to TP ratio of 1: 0.24, and the results from the tracer analysis yielded a ratio of 1: 0.23. Based on the sensitivity of the TP test, it is unlikely that the small decrease in TP was significant. The amended water for the tracer test had a Br^- to NO_3^--N ratio of 1: 1.20, and the results from the tracer test yielded a ratio of 1: 1.215 – 1.254. The increase of NO_3^--N shown in the analysis is not assumed to be production of NO_3^--N, rather was a result of the sampling methodology. In conclusion, no loss of NO_3^--N was evident during the tracer test in the tile drain.

The temporal analysis of water quality patterns can be affected by advection, chemical diffusion/dispersion, and chemical reactions. At the scale of the tile drain tracer test, advection response time would be short, with a horizontal scale of 396 meters and a horizontal flow velocity of 0.07 m/sec, yielding a response time of 94 minutes. According to Sawatsky (2009), tracer tests performed near wells at the OITA provided a hydraulic conductivity ranging from 0.44 – 0.95 m/hour. The advection response time from the injection wells to discharge within the subsurface drain would be between 3.2 – 6.9 hours.

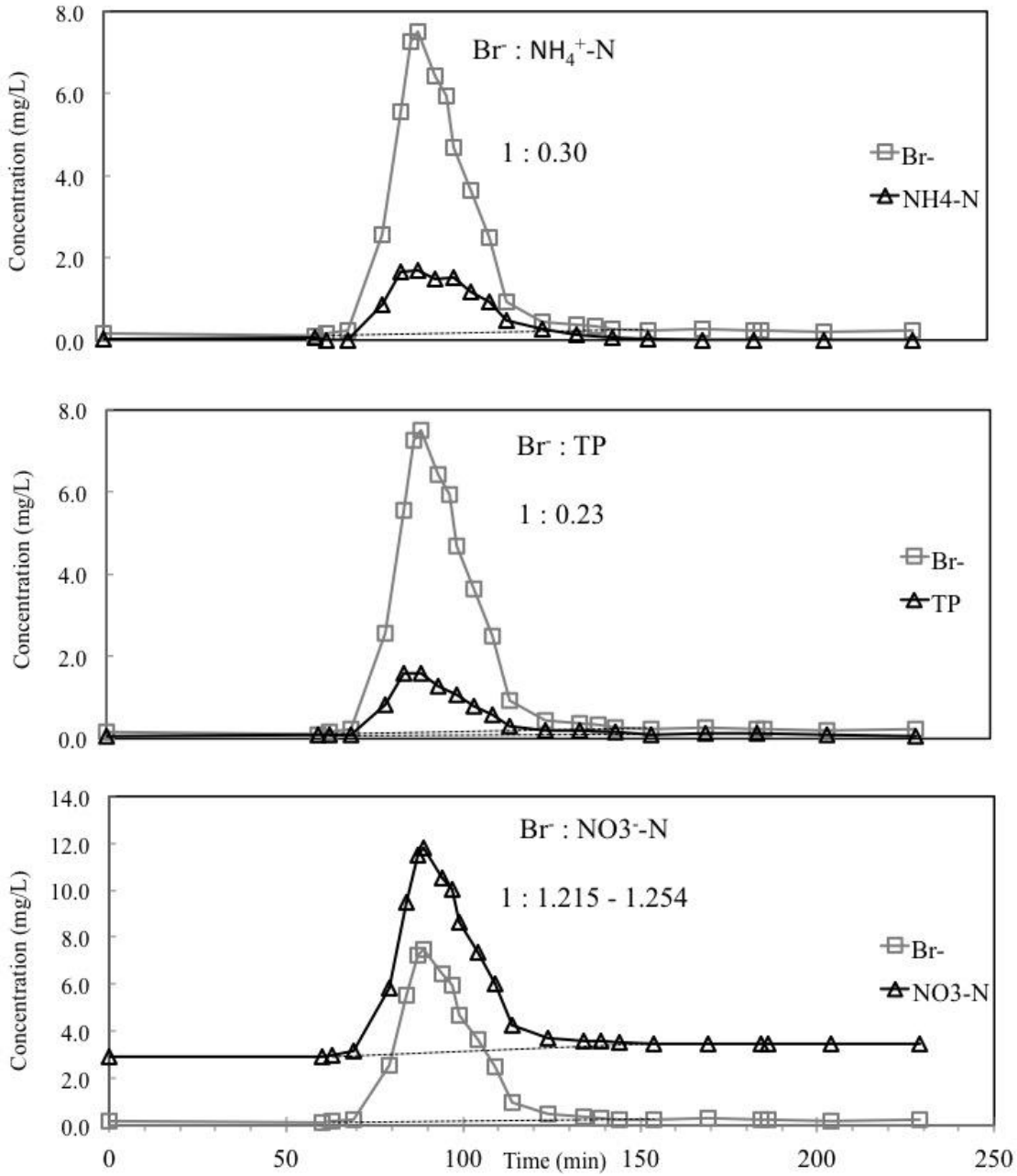

Figure 9. Comparison of analytes from tile drain tracer test.

Based on the data provided from the sediment analyses and the ISm tests in the gravel pack, we know that denitrification occurs within the imported gravel pack. Fetter (2001) lists between 0.36 to 36 m/hour as the range for hydraulic conductivities of well-sorted gravel. Using this range, the travel time within the gravel pack would be

between 18 minutes and 11 seconds until groundwater is discharged into the tile drains. Using the maximum zero-order denitrification rate from the ISm gravel pack tests of 0.296 mg/L/day, the gravel pack would reduce the nitrate concentration of groundwater entering the tile-drains by approximately 4 $x10^{-3}$ mg/L, which is too low to detect with the methodologies used herein.

CHAPTER V

CONCLUSIONS

A study of denitrification potential within multiple mediums was conducted in the Oakes Irrigation Test Area of southeastern North Dakota, and showed differences in their possible potential. Aquifer materials containing fine-grained materials had the highest amount of electron donors, and in-situ tracer tests performed in fine-grained aquifer materials exhibited the highest rate of NO_3^- attenuation. Both the electron donor analysis and the ISM tracer tests performed in aquifer sediments showed that finer-grained materials remove NO_3^- more quickly. The tile-drain tracer test indicated that the manganese biofilm present at this site have no significant effect on NO_3^- removal.

Organic carbon, inorganic sulfide, and ferrous iron were the substantial electron donors at the site, with no measureable quantity of organic sulfide present. Manganese was present the sedimentary facies at the site, however it was found to be concentrated within the tile drains and tile drain gravel pack. Organic carbon concentrations in silt-loam ranged from 0.44% to 0.74%, 0.09 % to 4.41% in sandy-loam, 0.06% to 0.40% in loamy-sand, and 0.03 to 1.664% in sand. The percentage of pyrite as inorganic sulfide (IS) was between 0.01% to 0.23% in combined silt-loam and silt. IS concentrations ranged between 0.01% to 0.17% in sandy-loam, 0.003% to 0.13% in loamy-sand, and 0.001% to 0.15% in sand. Ferrous iron concentrations ranged between 0.32% to 1.81% in silt and silt-loam combined, 0.10% to 0.89% in sandy-loam, 0.03% to 0.62% in loamy sand, and 0.15% to 0.64% in sand facies. Manganese was found in higher

concentrations within the three finer grained facies with concentrations ranging between 0.03% to 0.30%, whereas loamy-sand ranged between 0.003% to 0.12%, and sand between 0.003% and 0.10%. ISM-G1, which recorded the fastest rates of denitrification had a larger percentage of the e^- donor IS than ISM-C1. ISM-G1 also had larger percentages of e^- donors IS and Fe^{2+}.

Statistically significant correlations exist for various e- donors, showing a general increase in donor content as sediment size decreases. These results are similar to those of Maharjan's (2009) research involving electron donors and sediment size. The donors are also generally correlated with each other, indicating that if increased concentrations of one donor are found, it is likely that high concentrations of the other important donors will be found.

Results from the ISM/ISm tracer tests help to confirm the correlation between sediment size and denitrification potential. The denitrification rates for the two tracers tests performed in ISM-G1 were 0.59 and 0.28 mg/L/day. ISM-G1 was installed in a fine-grained loamy sand facies (Figure 8). The denitrification rates from the two tests performed in ISM-C1 were 0.061 mg/L/day and 0.033 mg/L/day. ISM-C1 was installed in a sand facies composed primarily of coarse and medium grained sands. The rates found in ISM-G1 were the highest rates measured amongst 25 denitrification tests conducted throughout the Midwest (Korom, personal communication), with ISM-C1 rates comparatively similar to previous tests. The elevated denitrification rates present within ISM-G1 suggest that any denitrification occurring at the site is occurring rapidly from within the fine-grained sediment facies. The textural analysis from ISM-G1 indicates that the ISM was installed in nearly 65% very fine-grained sand, with less

than 1% of the ISM-C1 sediment textures classified as larger than fine-grained sand. ISM-C1 was installed in primarily medium-grained sand (Figure 6). The sediments contained within ISM-C1 contain more electron donors by weight than the very fine-grained sands of ISM-G1 (Figure 5).Ism-C3 was installed in the gravel envelope, next to the tile drain near well nest C3. The denitrification rate measured in ISm-C3 measured was 0.11 mg/L/day. The tracer test within Ism-C3 showed evidence of heavy dilution by native groundwater. The ISm was later reinstalled in the tile drain gravel envelope next to well nest C7, resulting in less dilution from native groundwater. ISm-C7 recorded a zero-order denitrification rate of 0.30 mg/L/day, with a less reliable goodness of fit than that of ISm-C3. The increased size of the gravel in the gravel pack reduces the surface area, thus reducing the reactivity of the drains. The substantial denitrification in ISm-C7 is likely to be the result of manganese bacterial influences.

Within the tile drains, also congested with manganese biofilm, the results from the tracer test show no significant uptake of nutrients. The tracer test does indicate a slight production of NH_4^+, which was possibly exchanged with Na^+ during the amendment. It is suggested that future tile drain tracer tests provide analysis of all major cations, to further evaluate this hypothesis. Total phosphorus in the tile drains showed a slight decrease in concentration, which was considered insignificant or within analytical error. The amended water for the tracer test had a Br^- to NO_3^--N ratio of 1: 1.20, with the tracer test yielding a ratio of 1: 1.215–1.254. The increase of NO_3^--N shown in the analysis is not assumed to be production of NO_3^--N, rather inadequacies in the sampling methodology.

The results of the tile drain tracer tests, the ISM tracer tests, and the aquifer sediment analyses support the hypothesis that denitrification at the Oakes BMP site is occurring mainly within the aquifer sediments at the site and not from within the tile drains. It is concluded that the biomass within the drain tile did not react with or store NO_3^--N. Based on analyses of material from the tile drain gravel pack and from the tile drain biofilm, the tile drains are likely to have the chemical potential to remove NO_3^- via natural attenuation; however, retention times are too low for any denitrification to noticeably decrease nitrate concentrations in the drain effluent. Reducing the hydraulic retention time of the tile drain (and thereby reducing its hydraulic efficiency) may be necessary for it to serve as a functional in-line denitrification bioreactor.

APPENDICES

APPENDIX A
DETAILED METHODOLOGIES

Sampling Methods

Samples were collected in September of 2008 by coring the aquifer sediments at the study site. Eighteen potential sample locations were identified based on previous well logs. The United States Bureau of Reclamation's drill rig was used to collect the samples. Upon extraction from the subsurface, aquifer sediments were placed in glass jars, labeled and frozen until needed for analysis. After sampling was completed the holes were filled with source sediments. Several samples were collected from each site at varying intervals. Sampling locations and depths are reported in Table 5.

A total of ten sites yielded 43 samples. Additional samples from the tile drain gravel pack were collected during June and July of 2009. The samples taken closest to the surface are designated "A". The deepest sample from a location was designated "H". Facies were identified and divided in the field before freezing for later review.

Table 5

Name, Depth Interval, and Location for each Sampled Core. The Designation "A" Indicates the Sample Closest to the Ground Surface

Sample ID	Depth interval (ft below surface)	Sample Date
ISM-C1 A	9-10	9/25/2008
ISM-C1 B	10-12	
ISM-C1 C	12 (shale layer)	
ISM-C1 D	12-13	
ISM-C1 E	13-15	
ISM-C1 F	14	
ISM-C1 G	15-20	
ISM-C1 H	20-22	
C1.5 A	8-10	9/23/2008
C1.5 B	10-14	
C1.5 C	14-18	
C1.5 D	18-22	
C2.5 A	7-11	9/23/2008
C2.5 B	11-13	
C2.5 C	13-16	
C2.5 D	16-19	
C2.5 E	19-21	
C3.5 A	7-10	9/24/2008
C3.5 B	10-13	
C3.5 C	13-18	
C3.5 D	18-22	
C4.5 A	7-10	9/24/2008
C4.5 B	10-12	
C4.5 C	12-16	
C4.5 D	16-20	
C5.5 A	8-12	9/24/2008
C5.5 B	12-14	
C5.5 C	14-17	
C5.5 D	17-19	
C5.5 E	19-22	
C6.5 A	7-11	9/25/2008
C6.5 B	11-16	
C6.5 C	16-20	
C6.5 D	20-22	
C7.5 A	8-14	9/25/2008
C7.5 B	14-16	
C7.5 C	16-22	
C7.5 D	18-20	

Table 5 (continued)

Sample ID	Depth interval (ft below surface)	Sample Date
ISM-G1 A ISM-G1 B	13-15 15-18	7/30/2008
ISmC3GP	8	6/2/2009
ISmC3BGP	8	6/2/2009
48PSISmC3	8	6/3/2009
52PNISmC3	8	6/3/2009
ISmC7GP	8	6/3/2009
50PSISmC7	8	6/3/2009

Laboratory Analysis

Analysis consisted of inorganic sulfide analysis by the method of Canfield et al., (1986), a method for organic sulfide which Klapperich (2008) adapted from Tabatabai, (1996) and LaCount et al., (1998), total carbon analysis by the method of Churcher and Dickout, (1987), ferrous iron and manganese using a method of Kennedy et al., (1999) modified by Klapperich (2008) and a textural analysis adapted from USGS (2003) and ASTM (1998). Prior to analysis, all samples were thawed overnight in a refrigerator, ground to a fine powder with a mortar and pestle, and dried at 105° C for 24 hours. All chemical analyses were carried out at UND's Environmental Analytical Research Laboratory (EARL) under the supervision of the Lab Director.

Duplicates

When the percent difference of duplicate analyses was less than 25%, it was assumed that the results were reproducible and both values were kept. If percent difference was greater than 25%, the results were discarded for that sample. Results below detection limit were given the quantifiable detection limit value. The duplicate analyses for sediment facies are reported in Appendix B.

Inorganic Sulfide

The method of Canfield et al., (1986) was used to obtain measurements of inorganic sulfide. Approximately one gram of sample was subjected to a rigorous digestion process. Each sample was boiled for 1.75 hours with an acidified and reduced (via Jones Reductor) $CrCl_2$ solution that converts the inorganic sulfide to H_2S gas. A 3% zinc acetate solution collects the converted gas. This solution is then acidified with 35mL of 6 M HCl. Each step occurs within the presence of a nitrogen carrier gas and is

contained in sealed glassware. After acidification the solution is treated with a 1% starch solution and a commercially prepared 0.1 N iodine indicator solution. The quantity of S^- is then determined by back titration with 0.1 N sodium thiosulfate ($Na_2S_2O_3$) solution. According to Klapperich, (2008) this quantity is assumed to be predominately the mineral pyrite. Recovery of a pyrite standard averaged 95.4 ± 3.0% (n=5) (Appendix B).

The sodium thiosulfate solution is not perfectly equivalent in strength to the iodine solution so the $Na_2S_2O_3$ is titrated into a known quantity of iodine solution to calculate the equivalent difference. This should be done at least once every few days during an analysis run. The results of this test are reported as the I_2 ratio (Appendix B). The ratio is then applied to the quantity of $Na_2S_2O_3$ added to the sample solution to convert it to its equivalence as I_2. At this point the final calculations are made using Equation 2. This mass of S^- is compared to the original sample mass to find the percentage quantity.

Organic Sulfur

According to Tabatabai (1996) the occurrence of sulfur can take place in a variety of organic and inorganic forms. Organic sulfur is typically quantified as the difference between total S and inorganic S as SO_4^{2-} (Tabatabai, 1996). Klapperich, (2008) devised a simplified technique of analysis, using lab techniques available. Figure 2 in LaCount et al. (1998, page 6) notes that inorganic sulfates oxidize at temperatures above 600° C while organic sulfur compounds oxidize at a temperature range of 350° C to 425° C. The nearly two hour long exposure of the sample to a large quantity (20 mL) of concentrated HCl and a temperature of 100° C by the method of

Canfield et al. (1986) specifically targets inorganic sulfide. This method leaves behind insoluble sulfates and organic sulfides as the digestion effectively removes any soluble, inorganic S from the samples. Barite was the most common inorganic sulfate expected to survive the Canfield Method. Klapperich (2008) showed combustion of pure barite at 600° C went undetected by this method.

Organic sulfur analysis was conducted using the LECO SC-432 DR Sulfur Analyzer. Following the digestion of the sample via the method for inorganic sulfide (Canfield method), the sample was filtered, rinsed with deionized H_2 and dried for 24 hours at 104° C. The LECO Sulfur Analyzer was used to oxidize approximately 0.2g of the sample at a temperature of 600° C. The resulting sulfur readings are understood to be the result of OS. To produce a 0.5% organic sulfur standard, the EARL Laboratory director mixed the organic sulfur compound cystine ($C_6H_{12}N_2O_4S_2$) with an inert sediment sample.

Since a portion of the sample is removed in the processing stages, through acidification, reduction, and other losses, the final measured concentration must be adjusted to reflect the pre-treatment weight. This is done by dividing the measured concentration of OS by the quantity of 1 minus the percent of the material lost to treatment. Duplicate samples were run for each test and then averaged into a single value. Results from the analysis of a selection of 14 samples detected no organic sulfur within the sediment samples. Based on these results it was deemed unnecessary to continue on with organic sulfur analyses for the remaining samples.

Organic Carbon

The Shimadzu TOC-V_{CSN} Total Organic Carbon Analyzer and SSM-5000A were used for analysis of total organic carbon analysis by the method of Churcher and Dickout (1987). Samples were ground to a fine powder and inorganic carbon was removed by treatment with a 5% HCl acid solution for 24 hours. High levels of inorganic carbon can interfere with organic carbon measurements. Samples were then filtered, dried at 104° C for 24 hours, reground, and weighed to quantify the net inorganic carbon compound removed. The TOC-V_{CSN} then measures both inorganic carbon by acidification at 200° and total carbon by combustion at 960° C. Organic carbon concentration is then determined as difference between the two measurements. Standards of powdered carbonate ($CaCO_3$, 12% carbon) and glucose ($C_6H_{12}O_6$, 40% carbon) were used for inorganic and total organic carbon respectively.

Organic carbon results must be adjusted to reflect the pre-treatment sample weight, since a portion of the sample is lost to acidification. This is done in the same fashion as OS, where the measured value of OC is divided by the quantity of 1 minus the % carbonate removed, which accounts for the mass lost. All percentages of OC reflect this pre-treatment equivalence. Duplicate analyses have been performed on all samples, as combustion analysis is very sensitive and relatively rapid. Results from the duplicates are averaged to get a singular value for each sample. Complete results of OC analysis can be found in Appendix B.

Ferrous Iron

A modified method of Kennedy et al., (1999) was used to conduct ferrous iron analyses. This method calls for the sample to be treated with 5M HCl, boiled in a water

bath for one hour, and then shaken for a period of three days. Klapperich, (2008) found this method irreproducible and attempted to optimize the procedure by experimenting with varying methods. When the acid concentration was reduced and the reaction times, both in the bath and shaking time increased, the test became much more reliable.

Approximately 0.5 grams of dried and powdered sample was digested with 15mL of 1M HCl in a sealed vial. After boiling the solution in a water bath for a period of two hours it was then set on a rotator for seven days. The vial was centrifuged and the liquid extract analyzed by spectrophotometer. The HACH method 8446 for ferrous iron involves 1-10 phenathroline, which reacts with ferrous in the solution to produce an orange color. A dilution factor of 1000 was used to bring Fe(II) levels to within the range of the method. Recovery using a siderite ($FeCO_3$) standard averaged 91.3± 4.3% (n=6) (Appendix B). Ferrous iron percentage was calculated using Equation 2 from Tesfay (2006).

Manganese

The remaining liquid extract from the Fe(II) analyses was used to determine manganese within the sediments. The HACH method 8034 for manganese involves sodium periodate, which reacts with manganese in the solution to produce a violet color. Dilution factors between 5 and 50 were used to provide adequate sample for analysis. Recovery using a rhodochrosite ($MnCO_3$) standard averaged 84.9± 5.4% (n=6) (Appendix B). Manganese percentage was calculated in the same fashion as Fe(II), through use of Equation 2 from Tesfay (2006).

Textural Analysis

Following the method of textural analysis put forth in USGS (2003), sediment samples were divided into gravel (>2.0mm), very coarse sand (≤2.0 and >1.0mm), coarse sand (≤1.0 and >0.5mm), medium sand (≤0.5 and >0.25mm), fine sand (≤0.25 and >0.125mm), very fine sand (≤0.125 and >0.0625mm), silt (≤0.0625 and >0.004mm) and clay (≤0.004mm). The hydrometer method of sedimentation analysis determined particle sizes smaller than 0.0625mm, while a wet-sieve analysis classified those sediments larger than 0.0625mm (ASTM, 1998).

Particle sizes less than 0.0625 mm were determined by the hydrometer method of sedimentation analysis and sizes larger than 0.0625 mm were determined by wet-sieve analysis (ASTM, 1998). Sediment grains were divided into gravel (>2.0mm), sand ≤ 2.0 and > 0.0625 mm), silt (≤ 0.0625 mm and > 0.004 mm) and clay (≤ 0.004 mm). Sand particles were further differentiated into fine, medium and coarse (USGS, 2003). Some of the clay contents were found to be below the quantifiable detection limit (1%) and for the purpose of the statistical analysis, 1/2 the detection limit value was assigned to them. Only two samples were below the quantifiable detection limit for silt and one other was below the detection limit for gravel. We reported these quantities as 0%.

APPENDIX B
DETAILED RESULTS

Table 6

Inorganic Sulfide Analysis Results

Sample ID	Weight (mg)	I_2 ratio	A I_2 (mL)	B $N_2S_2O_4$ (mL)	C $N_2S_2O_4$ as I_2 (mL)	mg S^- (A-C)* 1.603	%S^- (mg S^- / mg samp*100)
ISM-C1 A	1002.0	1.0417	1.0	0.92	0.958	0.067	0.007
ISM-C1 B	1000.1	1.0381	1.0	0.90	0.934	0.105	0.011
ISM-C1 C	1000.9	1.0274	1.0	0.83	0.853	0.236	0.024
ISM-C1 D	1000.4	1.0345	1.0	0.94	0.972	0.044	0.004
ISM-C1 E	1000.6	1.0274	1.0	0.92	0.945	0.088	0.009
ISM-C1 F	999.6	1.0309	1.0	0.85	0.876	0.198	0.020
ISM-C1 G	1008.7	1.0274	1.0	0.78	0.801	0.318	0.032
ISM-C1 H	1008.2	1.0381	1.0	0.88	0.913	0.139	0.014
C1.5 A	1000.1	1.1152	1.0	0.91	1.015	0.000	0.000
C1.5 B	1028.7	1.0490	1.0	0.33	0.346	1.048	0.102
C1.5 C	1150.0	1.0526	2.0	0.75	0.789	1.940	0.169
C1.5 D	1045.4	1.0345	2.0	0.47	0.486	2.427	0.232
C2.5 A	1088.8	1.0345	1.0	0.95	0.983	0.028	0.003
C2.5 B	1404.7	1.0381	1.0	0.36	0.374	1.004	0.071
C2.5 C	1228.7	0.9934	1.0	0.21	0.209	1.269	0.103
C2.5 D	1022.2	0.9967	1.0	0.47	0.468	0.852	0.083
C2.5 E	1042.1	0.9934	1.0	0.72	0.715	0.456	0.044
C3.5 A	1018.0	1.0204	1.0	0.90	0.918	0.131	0.013
C3.5 B	1036.7	1.0239	2.0	0.96	0.983	1.630	0.157
C3.5 C	1059.4	0.9868	1.0	0.13	0.128	1.397	0.132
C3.5 D	1003.3	1.0000	2.0	0.60	0.600	2.244	0.224
C4.5 A	1131.1	1.0000	1.0	0.98	0.980	0.032	0.003
C4.5 B	1083.6	0.9967	1.0	0.62	0.618	0.612	0.057
C4.5 C	1023.3	1.0239	1.0	0.36	0.369	1.012	0.099
C4.5 D	1003.9	1.0204	1.0	0.42	0.429	0.916	0.091
C5.5 A	1011.1	1.0563	1.0	0.86	0.908	0.147	0.015
C5.5 B	997.3	1.0638	1.0	0.90	0.957	0.068	0.007
C5.5 C	1008.8	1.0870	1.0	0.48	0.522	0.767	0.076
C5.5 D	1012.1	1.0909	1.0	0.43	0.469	0.851	0.084
C5.5 E	1007.7	0.9615	1.0	0.26	0.250	1.202	0.119
C6.5 A	1004.9	1.0989	1.0	1.02	1.121	0.000	0.000
C6.5 B	1010.8	1.0239	1.0	0.32	0.328	1.078	0.107
C6.5 C	1009.0	1.0490	1.0	0.19	0.199	1.284	0.127
C6.5 D	997.4	1.0345	2.0	0.81	0.838	1.863	0.187
C7.5 A	996.6	1.0490	1.0	0.94	0.986	0.022	0.002
C7.5 B	1002.0	1.0601	1.0	0.82	0.869	0.210	0.021
C7.5 C	1010.0	1.0381	2.0	1.10	1.142	1.376	0.136
C7.5 D	999.5	1.0453	1.0	0.07	0.073	1.486	0.149

Table 6 (continued)

Sample ID	Weight (mg)	I_2 ratio	A I_2 (mL)	B $N_2S_2O_4$ (mL)	C $N_2S_2O_4$ as I_2 (mL)	mg S^- (A-C)* 1.603	%S^- (mg S^- / mg samp*100)
C8.5 A	1002.2	1.0830	1.0	0.92	0.996	0.006	0.001
C8.5 B	1006.2	1.1070	1.0	0.44	0.487	0.822	0.082
C8.5 C	1006.3	1.1152	1.0	0.19	0.212	1.263	0.126
ISM-G1 A	992.0	1.1450	1.0	0.37	0.424	0.924	0.093
ISM-G1 B	1001.7	1.1628	1.0	0.92	1.070	0.000	0.000
ISmC3GP	972.4	1.0563	1.0	0.88	0.930	0.113	0.012
ISmC3BGP	991.7	1.0526	1.0	0.95	1.000	0.000	0.000
48PSISmC3	1009.5	1.0526	1.0	0.81	0.853	0.236	0.023
52PNISmC3	1009.3	1.0526	1.0	0.92	0.968	0.051	0.005
ISmC7GP	1042.3	1.0601	1.0	0.93	0.986	0.023	0.002
50PSISmC7	1013.2	1.0714	1.0	0.93	0.996	0.006	0.001

Table 7

Inorganic Sulfide Analysis Pyrite Recoveries

Standards	Weight (mg)	I_2 ratio	A I_2 (mL)	B $N_2S_2O_4$ (mL)	C $N_2S_2O_4$ as I_2 (mL)	mg S^- (A-C)* 1.603	% Recovery
Pyrite	10.4	1.0239	4.0	0.57	0.584	5.476	98.5
Pyrite	10.1	1.0601	4.0	0.69	0.731	5.239	97.1
Pyrite	15.7	0.9934	5.0	0.09	0.089	7.872	93.8
Pyrite	11.0	0.9934	4.0	0.67	0.666	5.435	90.9
Pyrite	10.4	1.0204	4.0	0.63	0.643	5.382	96.8
Pyrite	10.3	1.0638	4.0	0.59	0.628	5.406	98.2
Pyrite	9.4	1.0526	3.0	0.11	0.116	4.623	92.0
						Average	= 95.3

Table 8

Organic Carbon Analysis Results. Columns Labeled 1 and 2 Represent Duplicates of Each Sample. OC is Calculated by Subtracting the IC Value from the TOC Value. Negative IC Values are Reported as Zero. Average OC is the Average Value of the Duplicates OC 1 and OC 2. TC – Total Carbon, IC – Inorganic Carbon, OC – Organic Carbon

Sample ID	TC 1	TC 2	TC Avg	IC 1	IC 2	IC Avg	OC 1	OC 2	OC Avg
ISM-C1 A	0.090	0.085	0.088	0.001	0	0.001	0.089	0.085	0.087
ISM-C1 B	0.060	0.075	0.068	0.001	0	0.001	0.059	0.075	0.067
ISM-C1 C	0.110	0.099	0.105	0.002	0	0.001	0.108	0.099	0.104
ISM-C1 D	0.068	0.078	0.073	0	0	0.000	0.068	0.078	0.073
ISM-C1 E	1.672	1.655	1.664	0	0	0.000	1.672	1.655	1.664
ISM-C1 F	1.176	1.196	1.186	0	0	0.000	1.176	1.196	1.186
ISM-C1 G	0.143	0.157	0.150	0	0	0.000	0.143	0.157	0.150
ISM-C1 H	0.552	0.562	0.557	0	0	0.000	0.552	0.562	0.557
C1.5 A	0.409	0.398	0.404	0	0	0.000	0.409	0.398	0.404
C1.5 B	0.312	0.312	0.312	0	0	0.000	0.312	0.312	0.312
C1.5 C	0.764	0.742	0.753	0	0	0.000	0.764	0.742	0.753
C1.5 D	0.730	0.748	0.739	0	0	0.000	0.730	0.748	0.739
C2.5 A	0.063	0.071	0.067	0	0	0.000	0.063	0.071	0.067
C2.5 B	0.154	0.117	0.136	0	0	0.000	0.154	0.117	0.136
C2.5 C	4.393	4.427	4.410	0	0	0.000	4.393	4.427	4.410
C2.5 D	2.090	2.112	2.101	0	0	0.000	2.090	2.112	2.101
C2.5 E	0.746	0.711	0.729	0	0	0.000	0.746	0.711	0.729
C3.5 A	0.178	0.182	0.180	0	0	0.000	0.178	0.182	0.180
C3.5 B	0.171	0.172	0.172	0	0	0.000	0.171	0.172	0.172
C3.5 C	0.452	0.435	0.444	0	0	0.000	0.452	0.435	0.444
C3.5 D	0.514	0.505	0.510	0	0	0.000	0.514	0.505	0.510
C4.5 A	0.026	0.028	0.027	0.008	0.007	0.008	0.018	0.021	0.020
C4.5 B	0.045	0.042	0.044	0.009	0.007	0.008	0.036	0.035	0.036
C4.5 C	0.100	0.110	0.105	0.010	0.008	0.009	0.090	0.102	0.096
C4.5 D	-0.007	0.078	0.036	0.009	0.008	0.009	0.000	0.070	0.035
C5.5 A	-0.008	0.055	0.024	0.010	0.009	0.010	0.000	0.046	0.023
C5.5 B	0.098	0.088	0.093	0.010	0.008	0.009	0.088	0.080	0.084
C5.5 C	0.371	0.358	0.365	0.008	0.008	0.008	0.363	0.350	0.357
C5.5 D	0.393	0.403	0.398	0.010	0.009	0.010	0.383	0.394	0.389
C5.5 E	0.746	0.725	0.736	0.009	0.009	0.009	0.737	0.716	0.727
C6.5 A	0.032	0.039	0.036	0	0	0.000	0.032	0.039	0.036
C6.5 B	0.093	0.088	0.091	0	0	0.000	0.093	0.088	0.091
C6.5 C	0.057	0.055	0.056	0	0	0.000	0.057	0.055	0.056
C6.5 D	1.013	1.010	1.012	0	0	0.000	1.013	1.010	1.012
C7.5 A	0.068	0.068	0.068	0	0	0.000	0.068	0.068	0.068
C7.5 B	0.357	0.365	0.361	0	0	0.000	0.357	0.365	0.361
C7.5 C	0.108	0.107	0.108	0	0	0.000	0.108	0.107	0.108
C7.5 D	0.175	0.162	0.169	0	0	0.000	0.175	0.162	0.169

Table 8 (continued)

Sample ID	TC 1	TC 2	TC Avg	IC 1	IC 2	IC Avg	OC 1	OC 2	OC Avg
C8.5 A	0.001	0.272	0.137	0.005	0.007	0.006	0.000	0.265	0.133
C8.5 B	0.070	0.070	0.070	0.003	0.007	0.005	0.067	0.063	0.065
C8.5 C	0.113	0.114	0.114	0.008	0.007	0.008	0.105	0.107	0.106
ISM-G1 A	0.223	0.221	0.222	0	0	0	0.223	0.221	0.222
ISM-G1 B	0.168	0.164	0.166	0	0	0	0.168	0.164	0.166
ISmC3GP	0.911	0.864	0.888	0	0	0	0.911	0.864	0.888
ISmC3BGP	0.408	0.418	0.413	0	0	0	0.408	0.418	0.413
48PSISmC3	1.236	1.150	1.193	0	0	0	1.236	1.150	1.193
52PNISmC3	1.493	1.477	1.485	0	0	0	1.493	1.477	1.485
ISmC7GP	0.731	0.715	0.723	0	0	0	0.731	0.715	0.723
50PSISmC7	0.371	0.369	0.370	0	0	0	0.371	0.369	0.370

Table 9

PT 1 and PT 2 are Calculated from OC 1 and OC 2 from Table 3 on Previous Page.
IC – Inorganic Carbon, PT – Pre-Treatment, AT – After Treatment, %Diff - % Difference

Sample ID	Mass PT	Mass filter	Mass At + Filter	Mass IC	IC % as xx-CO_3	PT eq (%C) 1	PT eq (%C) 2	% Diff
ISM-C1 A	5.1960	0.9703	5.6784	0.4879	9.39	0.0806	0.0770	2.299
ISM-C1 B	5.0312	0.9869	5.5750	0.4431	8.81	0.0538	0.0684	-11.940
ISM-C1 C	5.0117	0.9348	5.4952	0.4513	9.00	0.0983	0.0901	4.348
ISM-C1 D	5.0288	0.9597	5.5114	0.4771	9.49	0.0615	0.0706	-6.849
ISM-C1 E	5.0711	0.9775	5.3884	0.6602	13.02	1.4543	1.4395	0.511
ISM-C1 F	5.2109	0.9873	5.5399	0.6583	12.63	1.0274	1.0449	-0.843
ISM-C1 G	5.0527	1.0050	5.8158	0.2419	4.79	0.1362	0.1495	-4.667
ISM-C1 H	5.0286	1.0056	5.3405	0.6937	13.80	0.4759	0.4845	-0.898
C1.5 A	5.0710	0.9990	5.7174	0.3526	6.95	0.3806	0.3703	1.363
C1.5 B	5.2110	1.0017	5.8054	0.4073	7.82	0.2876	0.2876	0.000
C1.5 C	5.0530	0.9843	5.4914	0.5459	10.80	0.6815	0.6618	1.461
C1.5 D	5.0270	1.0161	5.1672	0.8759	17.42	0.6028	0.6177	-1.218
C2.5 A	5.1962	0.9989	5.8189	0.3762	7.24	0.0584	0.0659	-5.970
C2.5 B	5.1297	0.9707	5.6384	0.4620	9.01	0.1401	0.1065	13.653
C2.5 C	5.0780	1.0050	5.6388	0.4442	8.75	4.0087	4.0397	-0.385
C2.5 D	5.2863	0.9821	5.1258	1.1426	21.61	1.6383	1.6555	-0.524
C2.5 E	5.1035	0.9768	5.2828	0.7975	15.63	0.6294	0.5999	2.402
C3.5 A	4.7180	1.0024	5.3952	0.3252	6.89	0.1657	0.1695	-1.111
C3.5 B	5.2197	0.9826	5.7917	0.4106	7.87	0.1575	0.1585	-0.292
C3.5 C	5.8882	1.0033	6.1492	0.7423	12.61	0.3950	0.3802	1.917
C3.5 D	5.1243	0.9878	5.2530	0.8591	16.77	0.4278	0.4203	0.883

Table 9 (continued)

Sample ID	Mass PT	Mass filter	Mass At + Filter	Mass IC	IC % as xx-CO_3	PT eq (%C) 1	PT eq (%C) 2	% Diff
C4.5 A	5.1387	0.9752	5.6312	0.4827	9.39	0.0163	0.0190	-7.692
C4.5 B	5.2172	0.9994	5.7135	0.5031	9.64	0.0325	0.0316	1.408
C4.5 C	5.4075	0.9868	5.9600	0.4343	8.03	0.0828	0.0938	-6.250
C4.5 D	5.0857	0.9891	5.6512	0.4236	8.33	0.0000	0.0642	-100.000
C5.5 A	5.2912	0.9996	5.9488	0.3460	6.54	0.0000	0.0430	-
C5.5 B	5.5380	1.0081	6.0849	0.4612	8.33	0.0807	0.0733	100.000
C5.5 C	5.2602	0.9994	5.9016	0.3580	6.81	0.3383	0.3262	4.762
C5.5 D	5.3110	1.0041	5.9233	0.3928	7.40	0.3547	0.3649	1.823
C5.5 E	5.2873	0.9775	5.7301	0.5347	10.11	0.6625	0.6436	-1.416
								1.445
C6.5 A	5.5149	0.9655	6.0080	0.4724	8.57	0.0293	0.0357	-9.859
C6.5 B	5.4987	1.0058	5.9905	0.5140	9.35	0.0843	0.0798	2.762
C6.5 C	5.4158	1.0092	5.5705	0.8545	15.78	0.0480	0.0463	1.786
C6.5 D	5.0480	0.9483	5.1199	0.8764	17.36	0.8371	0.8347	0.148
C7.5 A	6.0982	0.9696	6.1752	0.8926	14.64	0.0580	0.0580	0.000
C7.5 B	5.5446	0.9763	6.0929	0.4280	7.72	0.3294	0.3368	-1.108
C7.5 C	6.0747	1.0203	6.5344	0.5606	9.23	0.0980	0.0971	0.465
C7.5 D	6.0838	0.9760	6.5323	0.5275	8.67	0.1598	0.1480	3.858
C8.5 A	5.2862	1.0120	6.0444	0.2538	4.80	0.0000	0.2523	-
C8.5 B	5.6777	0.9682	6.1693	0.4766	8.39	0.0614	0.0577	100.000
C8.5 C	5.3578	0.9776	5.8585	0.4769	8.90	0.0957	0.0975	3.077
								-0.943
ISM-G1 A	5.0406	0.9783	5.6280	0.3909	7.76	0.2057	0.2039	0.439
ISM-G1 B	5.0190	0.9841	5.6164	0.3877	7.72	0.1550	0.1513	1.208
ISmC3GP	1.0170	0.9888	1.5433	0.4625	45.48	0.4967	0.4711	2.648
ISmC3BGP	0.3034	0.9896	1.1774	0.1156	38.1	0.2525	0.2587	-1.211
48PSISmC3	2.1049	0.9912	2.3627	0.6434	31.93	0.8413	0.7828	3.604
52PNISmC3	0.6430	1.1394	1.5684	0.214	33.28	0.9961	0.9854	0.539
ISmC7GP	1.5006	1.0165	2.0715	0.4456	29.69	0.5139	0.5027	1.107
50PSISmC7	1.5089	0.9958	1.9227	0.582	38.57	0.2279	0.2267	0.27

Table 10

Fe(II) Extraction Analysis Results. Wt – Weight, AA – Amount Acid, BT – Boiling Time, RT – Rotation Time, DF – Dilution Factor, MR – Machine Reading

Sample ID	Weight (g)	Acid Conc.	AA (L)	BT (hr)	RT (dy)	DF	MR	% Fe(II)
ISM-C1 A	0.5009	1M	0.015	2	7	1000	0.03	0.090
ISM-C1 B	0.5071	1M	0.015	2	7	1000	0.01	0.030
ISM-C1 C	0.5043	1M	0.015	2	7	1000	0.11	0.327
ISM-C1 D	0.4907	1M	0.015	2	7	1000	0.05	0.153
ISM-C1 E	0.4966	1M	0.015	2	7	1000	0.10	0.302
ISM-C1 F	0.5061	1M	0.015	2	7	1000	0.09	0.267
ISM-C1 G	0.5006	1M	0.015	2	7	1000	0.10	0.300
ISM-C1 H	0.5090	1M	0.015	2	7	1000	0.54	1.591
C1.5 A	0.5093	1M	0.015	2	7	1000	0.11	0.324
C1.5 B	0.4943	1M	0.015	2	7	1000	0.15	0.455
C1.5 C	0.5039	1M	0.015	2	7	1000	0.19	0.566
C1.5 D	0.5092	1M	0.015	2	7	1000	0.04	0.118
C2.5 A	0.5070	1M	0.015	2	7	1000	0.04	0.118
C2.5 B	0.5060	1M	0.015	2	7	1000	0.07	0.208
C2.5 C	0.5051	1M	0.015	2	7	1000	0.15	0.445
C2.5 D	0.5159	1M	0.015	2	7	1000	0.28	0.814
C2.5 E	0.5048	1M	0.015	2	7	1000	0.18	0.535
C3.5 A	0.4980	1M	0.015	2	7	1000	0.14	0.422
C3.5 B	0.5072	1M	0.015	2	7	1000	0.10	0.296
C3.5 C	0.4977	1M	0.015	2	7	1000	0.18	0.542
C3.5 D	0.5047	1M	0.015	2	7	1000	0.21	0.624
C4.5 A	0.5003	1M	0.015	2	7	1000	0.01	0.030
C4.5 B	0.4912	1M	0.015	2	7	1000	0.11	0.336
C4.5 C	0.5065	1M	0.015	2	7	1000	0.18	0.533
C4.5 D	0.5089	1M	0.015	2	7	1000	0.16	0.472
C5.5 A	0.5080	1M	0.015	2	7	1000	0.06	0.177
C5.5 B	0.5051	1M	0.015	2	7	1000	0.16	0.475
C5.5 C	0.5076	1M	0.015	2	7	1000	0.19	0.561
C5.5 D	0.5062	1M	0.015	2	7	1000	0.18	0.533
C5.5 E	0.5058	1M	0.015	2	7	1000	0.18	0.534
C6.5 A	0.4977	1M	0.015	2	7	1000	0.05	0.151
C6.5 B	0.4953	1M	0.015	2	7	1000	0.16	0.485
C6.5 C	0.4996	1M	0.015	2	7	1000	0.16	0.480
C6.5 D	0.5032	1M	0.015	2	7	1000	0.55	1.640
C7.5 A	0.4984	1M	0.015	2	7	1000	0.04	0.120
C7.5 B	0.4898	1M	0.015	2	7	1000	0.13	0.398
C7.5 C	0.5040	1M	0.015	2	7	1000	0.14	0.417
C7.5 D	0.5015	1M	0.015	2	7	1000	0.17	0.508

Table 10 (continued)

Sample ID	Weight (g)	Acid Conc.	AA (L)	BT (hr)	RT (dy)	DF	MR	% Fe(II)
C8.5 A	0.5072	1M	0.015	2	7	1000	0.06	0.177
C8.5 B	0.4993	1M	0.015	2	7	1000	0.14	0.421
C8.5 C	0.5092	1M	0.015	2	7	1000	0.17	0.501
ISM-G1 A	0.5009	1M	0.015	2	7	1000	0.15	0.449
ISM-G1 B	0.4962	1M	0.015	2	7	1000	0.16	0.484
ISmC3GP	0.2552	1M	0.015	2	7	100	0.05	0.029
ISmC3BGP	0.1013	1M	0.015	2	7	100	0.04	0.059
48PSISmC3	0.2720	1M	0.015	2	7	100	0.25	0.138
52PNISmC3	0.2177	1M	0.015	2	7	100	0.26	0.179
ISmC7GP	0.2526	1M	0.015	2	7	25	0.11	0.016
50PSISmC7	0.2003	1M	0.015	2	7	100	0.06	0.045

Table 11

Fe(II) Extraction Analysis Standards Results. Standard is Siderite – 48.2% Fe(II). Wt – weight, AA – Amount Acid, BT – Boiling Time, RT – Rotation Time, DF – Dilution Factor, MR – Machine Reading

Standards	Weight (g)	Acid Conc.	AA (L)	BT (hr)	RT (dy)	DF	MR	Recovery (%)
Siderite	0.0119	1M	0.015	2	7	1000	0.36	94.2
Siderite	0.0105	1M	0.015	2	7	1000	0.30	88.9
Siderite	0.0110	1M	0.015	2	7	1000	0.32	90.5
Siderite	0.0097	1M	0.015	2	7	1000	0.29	93.0
Siderite	0.0122	1M	0.015	2	7	1000	0.38	96.9
Siderite	0.0092	1M	0.015	2	7	1000	0.25	84.6
Siderite	0.0930	1M	0.015	2	7	100	2.90	97.0
							Average	92.2
Pyrite	0.0134	1M	0.015	2	7	100	0.05	12.0
Pyrite	0.0162	1M	0.015	2	7	100	0.07	13.9
Pyrite	0.0096	1M	0.015	2	7	100	0.03	10.1
Pyrite	0.0178	1M	0.015	2	7	100	0.08	14.5
							Average	12.6

Table 12

Manganese Extraction Analysis Results. Wt – Weight, AA – Amount Acid, BT – Boiling Time, RT – Rotation Time, DF – Dilution Factor, MR – Machine Reading

Sample ID	Weight (g)	Acid Conc.	AA (L)	BT (hr)	RT (dy)	DF	MR	% Mn
ISM-C1 A	0.5009	1M	0.015	2	7	10	10.00	0.299
ISM-C1 B	0.5071	1M	0.015	2	7	5	6.00	0.089
ISM-C1 C	0.5043	1M	0.015	2	7	5	0.80	0.012
ISM-C1 D	0.4907	1M	0.015	2	7	5	2.30	0.035
ISM-C1 E	0.4966	1M	0.015	2	7	5	6.50	0.098
ISM-C1 F	0.5061	1M	0.015	2	7	5	1.30	0.019
ISM-C1 G	0.5006	1M	0.015	2	7	5	1.40	0.021
ISM-C1 H	0.509	1M	0.015	2	7	5	7.60	0.112
C1.5 A	0.5093	1M	0.015	2	7	5	4.60	0.068
C1.5 B	0.4943	1M	0.015	2	7	5	2.70	0.041
C1.5 C	0.5039	1M	0.015	2	7	5	5.40	0.080
C1.5 D	0.5092	1M	0.015	2	7	10	7.00	0.206
C2.5 A	0.5070	1M	0.015	2	7	5	3.20	0.047
C2.5 B	0.5060	1M	0.015	2	7	5	2.70	0.040
C2.5 C	0.5051	1M	0.015	2	7	5	4.40	0.065
C2.5 D	0.5159	1M	0.015	2	7	5	16.60	0.241
C2.5 E	0.5048	1M	0.015	2	7	5	4.90	0.073
C3.5 A	0.4980	1M	0.015	2	7	5	0.10	0.002
C3.5 B	0.5072	1M	0.015	2	7	5	2.40	0.035
C3.5 C	0.4977	1M	0.015	2	7	5	4.70	0.071
C3.5 D	0.5047	1M	0.015	2	7	5	10.80	0.160
C4.5 A	0.5003	1M	0.015	2	7	5	7.70	0.115
C4.5 B	0.4912	1M	0.015	2	7	5	3.10	0.047
C4.5 C	0.5065	1M	0.015	2	7	5	8.00	0.118
C4.5 D	0.5089	1M	0.015	2	7	5	3.70	0.055
C5.5 A	0.508	1M	0.015	2	7	5	6.80	0.100
C5.5 B	0.5051	1M	0.015	2	7	5	1.80	0.027
C5.5 C	0.5076	1M	0.015	2	7	5	2.30	0.034
C5.5 D	0.5062	1M	0.015	2	7	5	1.90	0.028
C5.5 E	0.5058	1M	0.015	2	7	5	0.30	0.004
C6.5 A	0.4977	1M	0.015	2	7	5	0.40	0.006
C6.5 B	0.4953	1M	0.015	2	7	5	0.20	0.003
C6.5 C	0.4996	1M	0.015	2	7	5	0.30	0.005
C6.5 D	0.5032	1M	0.015	2	7	5	7.40	0.110
C7.5 A	0.4984	1M	0.015	2	7	5	1.20	0.018
C7.5 B	0.4898	1M	0.015	2	7	5	3.40	0.052
C7.5 C	0.504	1M	0.015	2	7	5	4.30	0.064
C7.5 D	0.5015	1M	0.015	2	7	5	3.40	0.051

Table 12 (continued)

Sample ID	Weight (g)	Acid Conc.	AA (L)	BT (hr)	RT (dy)	DF	MR	% Mn
C8.5 A	0.5072	1M	0.015	2	7	5	1.60	0.024
C8.5 B	0.4993	1M	0.015	2	7	5	1.10	0.017
C8.5 C	0.5092	1M	0.015	2	7	5	3.60	0.053
ISM-G1 A	0.5009	1M	0.015	2	7	5	0.20	0.003
ISM-G1 B	0.4962	1M	0.015	2	7	5	3.00	0.045
ISmC3GP	0.2552	1M	0.015	2	7	25	22	3.233
ISmC3BGP	0.1013	1M	0.015	2	7	5	5.6	0.415
48PSISmC3	0.272	1M	0.015	2	7	5	8	0.221
52PNISmC3	0.2177	1M	0.015	2	7	5	6.4	0.22
ISmC7GP	0.2720	1M	0.015	2	7	5	8.00	0.221
50PSISmC7	0.2526	1M	0.015	2	7	5	2.8	0.083

Table 13

Manganese Extraction Analysis Standards Results. Standard is Rhodochrosite – 47.8% Manganese. Wt – Weight, AA – Amount Acid, BT – Boiling Time, RT – Rotation Time, DF – Dilution Factor, MR – Machine Reading

Standards	Weight (g)	Acid Conc.	AA (L)	BT (hr)	RT (dy)	DF	MR	Recovery (%)
Rhodochrosite	0.0106	1M	0.015	2	7	50	6.1	90.294
Rhodochrosite	0.0114	1M	0.015	2	7	50	5.7	78.452
Rhodochrsite	0.0092	1M	0.015	2	7	50	4.8	81.863
Rhodochrosite	0.0108	1M	0.015	2	7	50	5.9	85.716
Rhodochrosite	0.0087	1M	0.015	2	7	50	5.1	91.978
Rhodochrosite	0.0122	1M	0.015	2	7	50	6.3	81.024
Rhodochrosite	0.0121	1M	0.015	2	7	50	7.2	93.364
							Average	86.099

Table 14

Results of OITA Textural Analyses

Sample ID	Gravel (%)	Sand (%)						Silt (%)	Clay (%)
		Very Coarse	Coarse	Medium	Fine	Very Fine	Total		
ISM-C1 A	1.6	0.7	2.9	34.9	14.0	15.0	67.4	26.1	4.9
ISM-C1 B	0.0	0.4	0.7	3.2	35.1	45.7	85.1	11.3	3.5
ISM-C1 C	0.7	3.1	18.4	51.9	10.6	6.0	90.0	6.0	3.3
ISM-C1 D	1.1	0.6	12.6	55.2	18.6	4.7	91.9	3.9	3.2
ISM-C1 E	1.7	5.2	10.1	48.0	19.8	4.3	87.3	7.7	3.2
ISM-C1 F	1.4	4.1	13.2	47.5	19.2	4.8	88.8	7.5	2.3
ISM-C1 G	0.0	0.2	2.2	53.5	32.7	4.2	92.9	3.8	3.3
ISM-C1 H	0.6	0.6	1.6	6.4	8.2	5.4	22.2	72.3	5.0
C1.5 A	0.0	0.0	0.6	1.7	14.8	57.3	74.3	23.8	1.9
C1.5 B	0.0	0.0	0.2	1.3	20.1	61.3	82.8	14.7	2.5
C1.5 C	0.0	0.1	0.1	0.3	12.7	58.1	71.4	26.3	2.2
C1.5 D	4.8	2.3	3.7	7.4	10.6	11.0	35.0	51.1	9.2
C2.5 A	0.0	0.0	0.2	0.9	13.9	69.9	84.8	14.5	0.8
C2.5 B	0.5	0.3	3.1	8.7	42.0	33.1	87.2	9.9	2.4
C2.5 C	3.6	8.9	8.5	7.0	18.5	32.5	75.4	19.3	1.6
C2.5 D	10.3	14.2	28.7	17.3	6.6	7.9	74.6	13.1	2.1
C2.5 E	0.5	0.5	2.1	2.9	3.6	7.2	16.2	74.9	8.4
C3.5 A	0.0	0.0	0.2	1.8	38.4	48.7	89.1	8.9	2.0
C3.5 B	0.0	0.2	1.1	1.8	51.9	12.5	67.5	29.2	3.3
C3.5 C	0.2	0.2	0.9	5.1	8.3	29.2	43.6	53.2	3.0
C3.5 D	2.5	2.5	4.0	8.7	12.4	13.6	41.2	52.1	4.2
C4.5 A	0.0	0.0	0.2	1.2	56.2	25.8	83.4	13.6	3.0
C4.5 B	0.0	0.0	0.2	1.4	37.3	47.8	86.7	9.1	4.1
C4.5 C	0.0	0.0	0.0	4.6	42.0	38.1	84.7	11.9	3.3
C4.5 D	0.0	0.0	0.2	7.3	59.3	25.1	91.9	2.9	5.2
C5.5 A	0.0	0.0	0.2	4.3	59.0	31.0	94.5	1.4	4.1
C5.5 B	0.0	0.0	3.2	0.0	44.5	34.0	81.7	15.8	2.5
C5.5 C	0.0	0.0	7.7	0.0	35.3	21.5	64.5	30.0	5.5
C5.5 D	0.0	0.0	1.3	24.4	28.3	37.6	91.6	3.0	5.4
C5.5 E	1.8	2.3	11.7	23.5	17.8	31.2	86.5	8.4	3.4
C6.5 A	0.0	0.0	0.2	2.9	40.6	47.3	91.0	8.0	1.0
C6.5 B	0.0	0.0	0.0	1.0	39.6	41.6	82.2	15.7	2.0
C6.5 C	16.0	2.7	2.5	5.8	55.5	14.4	80.9	0.4	2.7
C6.5 D	0.0	0.0	0.0	0.3	0.6	1.1	2.0	93.7	4.3
C7.5 A	0.2	0.2	0.2	2.6	39.3	41.9	84.3	13.3	2.2
C7.5 B	0.0	0.0	0.2	8.9	35.9	32.5	77.5	20.3	2.2
C7.5 C	0.0	0.2	0.5	3.9	55.7	32.3	92.6	3.9	3.5
C7.5 D	0.2	0.2	0.2	4.1	38.6	47.4	90.4	6.3	3.0
C8.5 A	0.0	0.0	0.7	4.9	36.1	49.2	90.9	7.9	1.2
C8.5 B	0.0	0.0	0.0	0.4	11.0	77.1	88.6	9.3	2.1
C8.5 C	0.0	0.0	0.2	1.7	21.4	59.9	83.2	15.7	1.1
ISM-G1 A	0.0	0.0	0.1	0.8	24.3	63.9	89.1	5.7	5.1
ISM-G1 B	0.0	0.0	0.3	0.5	19.0	65.6	85.4	8.0	6.7

Table 15

Munsell Soil Color for OITA Sediments

Sample ID	Depth	Munsell soil color (moist sample)			
		Hue	Value	Chroma	Color
ISM-C1 A	9-10	2.5Y	3.0	/3	Dark olive brown
ISM-C1 B	10-12	2.5Y	3.0	/1	Very dark gray
ISM-C1 C	12 (shale layer)	2.5Y	3.0	/1	Very dark gray
ISM-C1 D	12-13	10YR	3.0	/6	Dark yellowish
ISM-C1 E	13-15	2.5Y	2.5	/1	Black
ISM-C1 F	14	2.5Y	2.5	/1	Black
ISM-C1 G	15-20	Gley 1	4.0	/10Y	Dark greenish
ISM-C1 H	20-22	Gley 1	3.0	/10Y	Very dark greenish gray
C1.5 A	8-10	2.5Y	4.0	/3	Olive brown
C1.5 B	10-14	Gley 1	4.0	/10Y	Dark greenish
C1.5 C	14-18	Gley 1	4.0	/N	Dark gray
C1.5 D	18-22	Gley 1	4.0	/10Y	Dark greenish gray
C2.5 A	7-11	10YR	4.0	/4	Dark yellowish
C2.5 B	11-13	Gley 1	4.0	/10Y	Dark greenish
C2.5 C	13-16	Gley 1	3.0	/10Y	Very dark
C2.5 D	16-19	Gley 1	3.0	/10Y	Very dark
C2.5 E	19-21	Gley 1	4.0	/10Y	Dark greenish gray
C3.5 A	7-10	10YR	3.0	/3	Dark brown
C3.5 B	10-13	Gley 1	4.0	/10Y	Dark greenish
C3.5 C	13-18	Gley 1	3.0	/10Y	Very dark
C3.5 D	18-22	Gley 1	4.0	/10Y	Dark greenish gray
C4.5 A	7-10	10YR	3.0	/4	Dark yellowish
C4.5 B	10-12	2.5Y	4.0	/2	Dark grayish
C4.5 C	12-16	Gley 1	4.0	/N	Dark gray
C4.5 D	16-20	Gley 1	4.0	/N	Dark gray
C5.5 A	8-12	2.5Y	4.0	/3	Olive brown
C5.5 B	12-14	10YR	3.0	/3	Dark brown
C5.5 C	14-17	Gley 1	4.0	/N	Dark gray
C5.5 D	17-19	Gley 1	4.0	/N	Dark gray
C5.5 E	19-22	Gley 1	4.0	/N	Dark gray
C6.5 A	7-11	10YR	3.0	/4	Dark yellowish
C6.5 B	11-16	Gley 1	4.0	/N	Dark gray
C6.5 C	16-20	2.5Y	5.0	/2	Grayish brown
C6.5 D	20-22	Gley 1	4.0	/10Y	Dark greenish gray
C7.5 A	8-14	2.5Y	4.0	/4	Olive brown
C7.5 B	14-16	Gley 1	4.0	/10Y	Dark greenish
C7.5 C	16-22	Gley 1	5.0	/10Y	Greenish gray
C7.5 D	18-20	Gley 1	5.0	/10Y	Greenish gray

Table 15. (continued)

Sample ID	Depth	Munsell soil color (moist sample)			
		Hue	Value	Chroma	Color
C8.5 A	8-12	2.5Y	4.0	/2	Dark grayish
C8.5 B	12-14	2.5Y	4.0	/2	Grayish brown
C8.5 C	14-22	Gley 1	5.0	/10Y	Greenish gray
ISM-G1 A	13-15	2.5Y	4.0	/2	Dark grayish
ISM-G1 B	15-18	2.5Y	3.0	/2	Very dark grayish brown

Table 16

Summary of the Results from the First Tile Drain Tracer Test

Time	Time (min	EC (uS/cm)	Time (cont.)	Time (min) (cont.)	EC (uS/cm) (cont.)
2:29:00	0	1068	4:27:00	82	1040
3:05:00	10	Injection	4:29:00	84	1049
3:15:00	13	1063	4:31:00	86	1065
3:18:00	16	1059	4:33:00	88	1087
3:21:00	19	1058	4:35:00	90	1107
3:24:00	22	1057	4:37:00	92	1120
3:27:00	25	1050	4:39:00	94	1128
3:30:00	28	1050	4:41:00	96	1131
3:33:00	31	1049	4:43:00	98	1133
3:36:00	34	1048	4:44:40	99	1132
3:39:00	37	1047	4:45:00	100	1132
3:42:00	40	1046	4:48:00	103	1131
3:45:00	43	1046	4:51:00	106	1130
3:48:00	46	1045	4:54:00	109	1129
3:51:00	49	1044	4:57:00	112	1126
3:54:00	52	1043	5:00:00	115	1123
3:57:00	55	1043	5:05:00	120	1120
4:00:00	58	1042	5:10:00	125	1118
4:03:00	61	1042	5:15:00	130	1115
4:06:00	64	1041	5:26:00	141	1107
4:09:00	67	1040	5:36:00	151	1097
4:12:00	70	1040	5:46:00	161	1085
4:15:00	73	1039	5:56:00	171	1068
4:18:00	76	1038	6:06:00	181	1049
4:21:00	79	1038	6:16:00	191	1036
4:24:00	0	1037	6:23:00	198	1030

Table 17

Summary of the Results from the Sample Analyses for the Second Tile Drain Test. Samples below Detection Limit (DL) were Analyzed as 0.50 of DL. Samples 5.5, 7.5, 13.5 and 17.5 were taken for Isotope Analysis (^{15}N and ^{18}O in NO_3^-) and were not Analyzed for TP or NH_4^+-N

Sample #	Time	Time (min)	Br^- (mg/L)	NO_3^--N (mg/L)	TP (mg/L)	NH_4^+-N (mg/L)
Tracer Start	9:26	0				
1	10:26	0	0.2	2.9	0.05	0.03
2	10:29	63	0.1	2.9	0.08	0.05
3	10:35	69	0.2	3.0	0.10	<0.01
4	10:45	79	0.2	3.1	0.08	<0.01
5	10:50	84	2.6	5.8	0.82	0.85
5.5	10:53	87	5.6	9.5	N/A	
6	10:55	89	7.3	11.5	1.60	1.66
7	11:00	94	7.5	11.8	1.60	1.69
7.5	11:03	97	6.4	10.5	N/A	
8	11:05	99	5.9	10.1	1.27	1.49
9	11:10	104	4.7	8.6	1.06	1.52
10	11:15	109	3.7	7.3	0.77	1.17
11	11:20	114	2.5	6.0	0.57	0.92
12	11:30	124	0.9	4.2	0.31	0.47
13	11:40	134	0.5	3.7	0.19	0.27
13.5	11:45	139	0.4	3.6	N/A	
14	11:50	144	0.3	3.6	0.20	0.14
15	12:00	229	0.3	3.5	0.15	0.08
16	12:15:20	169.333	0.2	3.5	0.09	0.01
17	12:30	184	0.3	3.5	0.13	<0.01
17.5	12:32	186	0.2	3.4	N/A	
18	12:50	204	0.2	3.5	0.12	<0.01
19	1:15	229	0.2	3.5	0.11	<0.01
20	1:45	229	0.2	3.5	0.07	<0.01

Table 18

Results of the Shapiro & Wilk "W-test" (Gilbert, 1987) for Normal Distribution of Electron Donor Data

Electron Donor	Ho NOT Rejected	Ho Rejected	Electron Donor	W	$W_{(0.05)*}$
Ln IS	X		Ln IS	0.955	0.947
IS		X	IS	0.861	0.947
Ln OC	X		Ln OC	0.979	0.947
OC		X	OC	0.612	0.947
Ln Fe		X	Ln FE	0.903	0.947
Fe		X	Fe	0.828	0.947
Ln Mn	X		Ln Mn	0.959	0.947
Mn		X	Mn	0.251	0.947

Ho: The population has a normal distribution
Ha: The population does not have a lognormal distribution

REFERENCES

American Society for Testing and Materials (ASTM), 1998. Standard test method for particle-size analysis of soils. Vol. 04.08.

Armstrong, C.A., 1980, Ground-water resources of Dickey and LaMoure Counties, North Dakota: County Ground-Water Studies No. 28, Part III, 61 p.

Ayars J.E. and K.K. Tanji. 1999. Effects of drainage water quality in arid and semiarid irrigated lands. Effects of inadequate drainage on crop growth and yield. In (Ed. R.W. Skaggs and J. van Schilfgaarde) Agricultural Drainage. Agronomy No. 38. American Society of Agronomy. Madison, Wi. Pp 831-870.

Bates, H.K., and R.F. Spalding. 1998. Aquifer denitrification as interpreted from in situ microcosm experiments. Journal of Environmental Quality 27, no. 1: 174–182.

Blann, K., J.L. Anderson, G.R. Sands, B. Bondracek. 2009. Effects of Agricultural Drainage on Aquatic Ecosystems: A Review. Critical Reviews of Science and Technology, 39:11, 909-1001.

Bluemle, J.P., 1979a. Geology of Dickey and LaMoure Counties: County Ground-Water Studies No. 28, Part I, 72 p.

Canfield, D.E., Raiswell, R., Westrich, J.T., Reaves, C.M., Berner, R.A. 1986. The use of chromium reduction in the analysis of reduced inorganic sulfur in sediments and shales. Chemical Geology. 54,149 – 155.

Casey, F.X.M., N. Derby, R.E. Knighton, D.D. Steele, and E.C. Stegman. 2002. Initiation of irrigation effects on temporal nitrate leaching. Vadose Zone j. 1:300-309.

Churcher, P.L., Dickout, R.D. 1986. Analysis of ancient sediments for total organic carbon – Some new ideas. Journal of Geochemical Exploration. 29 (2), 235 – 246.

Conover, W.J. 1971. Practical nonparametric statistics. Wiley, New York, 462.

Derby, N.E., R.E. Knighton, and D.D. Steele. 1997. Methods for monitoring leachate losses under irrigated corn best management practices. p. 243–257. *In* J. Schaak et al. (ed.) Proc. Water Manage. Conf., Fargo, ND. 16–19 July 1997. U.S. Committee on Irrig. and Drain., Denver, CO.

Derby, N.E., F.X.M. Casey, and R.E. Knighton. 2009. Long-term observations of vadose zone and groundwater nitrate concentrations under irrigated agriculture. Vadose Zone J. 8:290-300.

Derby, N.E., and R.E. Knighton. 2001. Field-scale preferential transport of water and chloride tracer by depression-focused recharge. J. Environ. Qual. 30:194-199.

Dinnes, D.L., D.L. Karlen, D.B. Jaynes, T.C. Kaspar, J.L. Hatfield, T.S. Colvin, and C.A. Cambardella. 2002. Nitrogen Management. Agron. J. 94, 153–171.

Downing, J.A., J.L. Baker, R.J. Diaz, T. Prato, N.N. Rabalais, and R.J. Zimmerman. 1999. Gulf of Mexico Hypoxia: Land-sea Interactions. Council for Agricultural Science and Technology Task Force Report No. 134. Ames, IA.

Eidman, V. 1997. Minnesota farmland drainage: Profitability and concerns. No. 688. Agricultural Economist. Available at http://purl.umn.edu/13165

Fetter, C.W. *Applied Hydrogeology, 4th Edition*. Prentice Hall, 2001. Print

Ford, H.W. 2005. Iron ochre and related sludge deposits in subsurface drain lines. Ext. Circ. 671. Florida Coop Ext., Univ. Florida, Gainesville.

Framji, K.K. and Mahajan, I.K. 1969. Irrigation and drainage in the world: a global review, Volume 1. Int. Comm. On Irrigation and Drainage.

Fraser, H., and Fleming, R. 2001. Environmental benefits of tile drainage-literature review. Prepared for Land Improvement Contractors of Ontario, University of Guelph, Ontario, Canada.

Frietag, Arden, and Dale Esser. 1986. Artificial recharge and drainage management in the Oakes Test Area. ASCE North American Water and Environment Congress. Anaheim, CA. June 22-28.

Gilbert, R.O. 1987. Statistical methods for environmental pollution monitoring. John Wiley and Sons, New York, 320.

Gillham, R.W., R.C. Starr, and D.J. Miller. 1990. A device for in situ determination of geochemical transport parameters, 2. Biochemical reactions. Ground Water 28, no. 6: 858–862.

Gilliam, J.W., J.L. Baker, and K.R. Reddy. 1999. Chapter 24: Water Quality Effects of Drainage in Humid Regions. In: R.W. Skaggs and J. van Schilfgaarde eds. Agricultural Drainage. Agron. Monogr. 38. American Society of Agronomy, Inc., Crop Science Society of America, Inc., Soil Science Society of America, Inc., Madison, Wisconsin, USA, Pp. 801-830.

Grass, L.B., A.J. Mackenzie and L.S. Willardson. 1976. Inspecting and cleaning subsurface drain systems. USDA-ARS Farmers Bull. 2258. U.S. Gov. Print Office, Washington, DC.

Green, C.T., Puckett, L.J., Böhlke, J.K., Bekins, B.A., Phillips, S.P., Kauffman, L.J., Denver, J.M., Johnson, H.M., 2008. Limited occurrence of denitrification in four shallow aquifers in agricultural areas of the United States. J. Environ. Qual. 37 (3), 994– 1009.

Hey, D.L. 2001. Modern drainage design: the pros, the cons, and the future. Hydrologic science: Challenges for the 21st century, Presentation at the 2001 Annual Meeting of the American Institute of Hydrology, Bloomington, MN.

Howarth, R.W., G. Billen, D. Swaney, A. Townsend, N. Jaworski, K. Lajtha, J.A. Downing, R. Elmgren, N. Caraco, T. Jordan, F. Berendse, J. Freney, V. Kudeyarov, P. Murdoch, and Z. Zhao-Liang. 1996. Regional nitrogen budgets and riverine N and P fluxes for the drainages to the North Atlantic Ocean: natural and human influences. Biogeochemistry 35, 575–139.

Ivarson, K.C. and Sojak, M. 1978. Microorganisms and ochre deposits in field drains of Ontario. Can. J. Soil Sci. 58: 1-17.

Kennedy, L.G., Everett, J.W., Ware, K.J., Parsons, R., Green, V. 1999. Iron and sulfur mineral analyses methods for natural attenuation assessments. Bioremediation Journal. 2, 259-276.

Knighton, R.E. 1997. Nitrate stratification in sand plain ground water systems under irrigation. Final Rep. Dep. Of Soil Scil, North Dakota State Univ., Fargo.

Korom, S.F. 1992. Natural denitrification in the saturated zone: A review. Water Resources Research. 28 (6), 1657-1668.

Korom, S.F., Schlag, A.J., Schuh, W.M., Schlag, A.K. 2005. In situ mesocosms: Denitrification in the Elk Valley Aquifer. Ground Water Monitoring and Remediation. 25 (1), 79-89.

Korom, S.F., Schuh, W.M., Tesfay, T., Spencer, E.J. 2012. Aquifer denitrification and in situ mesocosms: Modeling electron donor contributions and measuring rates. Journal of Hydrology. 432-433. 112-126.

Maharjan, B. 2009. MS Thesis: Correlation of electron donor concentrations in sediments with sediment properties: New Providence, Iowa. Department of Geology and Geological Engineering, University of North Dakota, Grand Forks, North Dakota.

McIsaac, G.F. and X. Hu. 2004. Net N input and riverine N export from Illinois agricultural watersheds with and without extensive tile drainage. Biogeochemistry 70, 253-273.

LaCount, R.B., Kern, D.G., Shriver, J.S., Banfield, T.L. 1997. Characterization of carbon in fly ash using Controlled-Atmosphere Programmed-Temperature Oxidation (CAPTO). Proceedings of the third annual conference on unburned carbon utility fly ash. US Department of Energy, FETC, 67.

Nodak Electric. 2011. Miles of Tile: Wet conditions set off drain tile boom in the Valley. The Nodak Neighbor. September/October 2011.

Pavelis, G.A. (ed.). (1987). *Farm drainage in the United States: History, status, and prospects*. Economic Research Service, USDA Misc. Publ. No. 1455, Washington, D.C.

Rabalais, N. N., R. E. Turner, D. Justic, Q. Dortch, W. J. Wiseman, Jr. and B. K. Sen Gupta (1996) Nutrient changes in the Mississippi River and system responses on the adjacent continental shelf. Estuaries 19(2B): 386-407.

Randall, G.W. and D.J. Mulla. 2001. Nitrate Nitrogen in surface waters as influenced by climatic conditions andagricultural practices. J. Environ. Qual. 30, 337–344.

Robinson, M. (1990). Impact of improved land drainage on river flows. Instutude of Hydrology Report No. 113. Center for Ecology and Hydrology, Edinburgh, U.K.

Robinson, M. and Rycroft, D.W. (1999). The impact of drainage on stream flows. Agron. Monogr., 38, 767-800.

Rowe, R.K., and VanGulck, J.F. 2004. Filtering and drainage of contaminated water. Keynote lecture, 4th International Conference on GeoFilters, Stellenbosch, South Africa, October, University of Witswatersrand, A.Fourie (Ed), pp1-63.

Salinas Klapperich, R.J., 2008. MS Thesis: Electron donor potential of Eastern North Dakota shale formations. Department of Geology and Geological Engineering, University of North Dakota, Grand Forks, North Dakota

Sawatzky, D.A., 2009. MS Thesis: Hydraulic efficiency in biofilm affected tile drains.

Schlag, A.J., 1999. In-situ Measurement of Denitrification in the Elk Valley Aquifer, Master's Thesis. Department of Geology and Geological Engineering, University of North Dakota, Grand Forks, North Dakota, 104p.

Schoonen, M.A.A. 2004. Mechanisms of sedimentary pyrite formation. In Amend, J.P., Edwards, K.J., Lyons, T.W. eds. Sulfur biogeochemistry-Past and Present. Boulder, Colorado, Geological Society of America Special Papers, 379, 117-134.

Schuh, W.M. 2008. Potential effects of subsurface drainage on water appropriation and the beneficial use of water in North Dakota. Water Resources Investigation No. 45. North Dakota State Water Commission. Bismarck, ND. 95 pp.

Sims, J.T., Simard, R.R., and Joern, B.C. (1998). Phosphorus loss in agricultural drainage: Historical perspective and current research. *J. Environ. Qual.,* 27, 277–29.

Spaling, H., and Smit, B. 1995. Conceptual model of cumulative environmental effects of agricultural land drainage. Agr. Ecosyst. Environ., 53, 299-308.

Starr, R.C., Gillham, R.W. 1993. Denitrification and organic carbon availability in two aquifers. Groundwater. 31 (6), 934-947.

Tabatabai, M.A. 1996. Sulfur. in Bartels, J.M., Bigham, J.M. eds. Methods of Soil Analysis Part 3 – Chemical Methods. Madison WI, Soil Science Society of America Inc, 921 – 960.

Tesfay, T., 2006. Dissertation: Modeling groundwater denitrification by ferrous iron using PHREEQC.

U.S. Bureau of Reclamation. Reclamation. Managing Water in the West. *Management of agricultural tile drains influences by manganese deposits and insights into other biofilm issues. Effects of iron bacteria on subsurface tile drains: influence on hydraulic efficiency and nutrient transport*. Kammer, A.K., Korom, S.F., Casey, F.X.M. 2009.

USGS website: http://pubs.usgs.gov/of/2003/of03-001/htmldocs/images/chart.gif http://ia.water.usgs.gov/nawzq/eiwa_ACT.html.